CLIMATE SCENARIOS FOR CALIFORNIA

DRAFT

A Report From:
California Climate Change Center

Prepared By:
Dan Cayan, Ed Maurer, Mike Dettinger, Mary Tyree, Katharine Hayhoe, Celine Bonfils, and Phil Duffy, Ben Santer

WHITE PAPER

DISCLAIMER

This report was prepared as the result of work sponsored by the California Energy Commission (Energy Commission) and the California Environmental Protection Agency (Cal/EPA). It does not necessarily represent the views of the Energy Commission, Cal/EPA, their employees, or the State of California. The Energy Commission, Cal/EPA, the State of California, their employees, contractors, and subcontractors make no warrant, express or implied, and assume no legal liability for the information in this report; nor does any party represent that the uses of this information will not infringe upon privately owned rights. This report has not been approved or disapproved by the California Energy Commission or Cal/EPA, nor has the California Energy Commission or Cal/EPA passed upon the accuracy or adequacy of the information in this report.

Arnold Schwarzenegger, *Governor*

December 2005
CEC-500-2005-203-SD

Acknowledgements

We acknowledge the international modeling groups for providing their data for analysis, the Program for Climate Model Diagnosis and Intercomparison (PCMDI) for collecting and archiving the model data, the JSC/CLIVAR Working Group on Coupled Modelling (WGCM) and their Coupled Model Intercomparison Project (CMIP) and Climate Simulation Panel for organizing the model data analysis activity, and the IPCC WG1 TSU for technical support. The IPCC Data Archive at Lawrence Livermore National Laboratory is supported by the Office of Science, U.S. Department of Energy. And, in particular, we thank the NOAA Geophysical Fluids Dynamics Laboratory global modeling group, and the NCAR/DOE Parallel Climate Modeling group for very responsive model output and consultation. Thanks to Alexander Gershunov for discussions and review of this manuscript. Thanks to Gregg Garfin, Phil Mote, and Kelly Redmond for careful and thoughtful reviews.

Preface

The Public Interest Energy Research (PIER) Program supports public interest energy research and development that will help improve the quality of life in California by bringing environmentally safe, affordable, and reliable energy services and products to the marketplace.

The PIER Program, managed by the California Energy Commission (Energy Commission), annually awards up to $62 million to conduct the most promising public interest energy research by partnering with Research, Development, and Demonstration (RD&D) organizations, including individuals, businesses, utilities, and public or private research institutions.

PIER funding efforts are focused on the following RD&D program areas:

- Buildings End-Use Energy Efficiency
- Energy-Related Environmental Research
- Energy Systems Integration
- Environmentally Preferred Advanced Generation
- Industrial/Agricultural/Water End-Use Energy Efficiency
- Renewable Energy Technologies

The California Climate Change Center (CCCC) is sponsored by the PIER program and coordinated by its Energy-Related Environmental Research area. The Center is managed by the California Energy Commission, Scripps Institution of Oceanography at the University of California at San Diego, and the University of California at Berkeley. The Scripps Institution of Oceanography conducts and administers research on climate change detection, analysis, and modeling; and the University of California at Berkeley conducts and administers research on economic analyses and policy issues. The Center also supports the Global Climate Change Grant Program, which offers competitive solicitations for climate research.

The California Climate Change Center Report Series details ongoing Center-sponsored research. As interim project results, these reports receive minimal editing, and the information contained in these reports may change; authors should be contacted for the most recent project results. By providing ready access to this timely research, the Center seeks to inform the public and expand dissemination of climate change information; thereby leveraging collaborative efforts and increasing the benefits of this research to California's citizens, environment, and economy.

For more information on the PIER Program, please visit the Energy Commission's website www.energy.ca.gov/pier/ or contact the Energy Commission at (916) 654-5164.

Table of Contents

Preface ii
Abstract vii
1.0 Introduction 1
2.0 Climatological Characteristics in California: Observational Criteria 1
3.0 Natural Variability vs. Climate Forcing 2
4.0 Scenarios and Models Selected 3
5.0 Characteristics of Model Simulations 3
6.0 Bias Correction and Spatial Downscaling of GCM Output 6
7.0 Hydrologic Modeling 8
8.0 References 10

List of Tables

Table 1. Temperature and Precipitation Changes, GFDL and PCM B1 and A2 simulations, Northern and Southern California. Temperature units are °C, precipitation in mm. Mean values are provided for historical (1961-1990) period, and changes between successive 30year periods are shown in subsequent columns for the models/emission scenarios, as indicated. 15

Table 2a. Seasonal temperature occurrences in historical tercile classes, Northern California. Temperature units are °Celsius. σ is standard deviation, μ is mean, T1 and T2 are lower and upper tercile thresholds of (1961-1990) historical distribution, n1 is median, N1 is number of seasons within period whose mean temperature falls into lower tercile of (1961-1990) distribution; N1+N2 is number falling into lower and middle terciles of (1961-1990) distribution. 16

Table 2b. Seasonal temperature occurrences in historical tercile classes, Southern California. Temperature units are °Celsius. σ is standard deviation, μ is mean, T1 and T2 are lower and upper tercile thresholds of (1961-1990) historical distribution, n1 is median, N1 is number of seasons within period whose mean temperature falls into lower tercile of (1961-1990) distribution; N1+N2 is number falling into lower and middle terciles of (1961-1990) distribution. 17

Table 3. Change in April 1 snow accumulation, San Joaquin, Sacramento, and parts of Trinity drainages from VIC hydrologic model. Similar computations for HadCM3 A1fi and B1 simulations and for PCM A1fi simulation are presented in Table 1 of Hayhoe et al., 2004..18

List of Figures

Figure 1. Observed and modeled precipitation, Northern and Southern California 19

Figure 2. Tropical Pacific sea surface temperature (SST), Nino 3.4 region, GFDL and PCM historical simulations, and NOAA CPC observations, 1950-2000. 20

Figure 3. Correlation between Nino 3.4 SST and precipitation across the globe from simulations GFDL (above) and PCM (middle), along with observations from NCEP/NCAR Reanalysis www.cdc.noaa.gov/cdc/reanalysis/reanalysis.shtml (below) demonstrate reasonably strong connection between tropical Pacific ENSO fluctuations and extratropical precipitation. 21

Figure 4a. 10-year running average of temperature anomalies (deg C) for California relative to the 1961-1990 base period average using annual (black), winter (blue),spring (green), summer (red), fall (brown) means. The time-series are computed from the UW monthly 1/8-degree gridded meterological dataset. 22

Figure 4b. Estimated natural variability of California temperature without forcing (bars), and observed temperature change (dots) during the 1950-2000 historical record. 22

Figure 5. Climate sensitivity as gaged by difference in simulated gobal temperature over California. There are two runs each for GFDL (GFDL 0 and GFDL 1), and PCM (PCM2 and PCM3). 23

Figure 6. GHG (CO_2) emissions (above) and atmospheric concentrations (below) prescribed by IPCC for several emissions scenarios, including B1, A2 and A1Fi. 24

Figure 7. Global precipitation for January and July from Reanalysis (model version of observations), PCM, and GFDL historical model runs 25

Figure 8. Projected Precipitation 2070-2099, Northern and Southern California. Compare with GCM historical and observed precipitation in Figure 1. 26

Figure 9. Correlations between Nov-Mar mean precipitation, Northern California, and Nov-Mar 500HPa height anomalies at each point in Pacific-western North America domain for (1961-1990) historical period and for 2070-2099 of GFDL and PCM A2 simulations, and for observations from NCAR/NCEP Reanalysis. 27

Figure 10. Joint Probability Distribution, Temperature and Precipitation Change 2070-2099, constructed from ensemble of IPCC AR4 model simulations. This shows, from a sampling of a collective of three different emissions scenarios run by 13 different global climate

models, the probability of a given pairing of changes of temperature and precipitation in 2070-2099 relative to their historical means during 1961-1990. Isopleths define loci of points having equal probability, as labeled. Superimposed upon the matrix of joint probablilities are specific results considered in the present Scenarios Project: GFDL CM2.1 (G), PCM (P), and HadCM3 (H) models, under emission scenarios B1 (b), A2 (a), and A1fi (f) are labeled. 28

Figure 11. Distribution of changes in Northern California temperature (in ^{o}C, above) and precipitation (in %, below) constructed from a sampling technique (Dettinger 2005) applied to recent set of IPCC 4th Assessment climate simulations, 13 models, 3 GHG emission scenarios). The temperature change plot shows that, by 2070-2099, virtually all simulations experience warming, by a broad range of amounts, but with a mean value of about +3C. On the other hand, concerning precipitation there are nearly as many simulations that become wetter as those that become drier, although by 2070-2099, there is a slight concensus to become drier, with the mean and most frequent value of precipitation change to be a decrease of just a few percent of its historical mean. Distributions are shown for 3 time blocks: 2005-2034, 2035-2064, and 2070-2099. The changes exhibited by the PCM and GFDL A2 and B1 simulations used in this study are indicated, for comparison with the entire family of climate projections. 29

Figure 12a. Ensemble of Northern California temperature projections from 39 AR4 model simulations with PCM (left) and GFDL (right) B1 and A2 runs highlighted Note that models are coupled ocean atmosphere GCM's, and while they are driven by external forcings such as solar variability, volcanic aerosols, greenhouse gases and anthopogenic aerosols, they are not guided by ocean surface temperature or atmospheric circulation patterns that would allow them to replicate the actual observed climate variability during the historical period. 30

Figure 12b. Ensemble of Northern California precipitation projections from 39 AR4 model simulations with PCM (left) and GFDL (right) B1 and A2 runs highlighted 31

Figure 13a. Northern California Temperature Variability between four ensemble members, PCM A2 simulations, with simulation used in this study highlighted. 32

Figure 13b. Northern California Precipitation Variability between four ensemble members, GFDL A2 simulations, with simulation used in this study highlighted 33

Figure 14. Temperature change from GFDL A2 simulation (right), and downscaled temperatures for (1961-1990) and (2070-2099) using Wood et al. statistical scheme (left). ... 34

Figure 15. California precipitation 2070-2099, 1961-1990 and change from PCM (above) and high resolution representation from VIC statistical downscaling (below) for JJA and DJF.. 35

Figure 16. Distribution, binned by 1°C intervals, of daily minimum temperature (Tmin) on days when precipitation is in upper, middle, lower tercile of daily precipitation amounts that exceed "drizzle" category, in addition to days with zero precipitation from GFDL A2 (left)

and B1 (right) simulations. Open and red bars show contribution to frequency distributions from historical (1961-1990) and (2070-2099) periods, respectively. Frequency bins lower than -10C and greater than +10ºC are omitted. 36

Figure 17. California Statewide April 1 Snow Water Equivalent Averages from Historical, 2005-2034, 2035-2064, 2070-2099 GFDL A2, PCM A2, GFDL B1 and PCM B1 simulations .. 37

Figure 18. California Statewide April 1 Snow Water Equivalent GFDL A2, PCM A2, GFDL B1 and PCM B1 simulations 38

Figure 19. Change in spring snow accumulation from VIC, as driven by climate changes from four different climate change simulations. Changes are expressed as. ratio of 2070-2099 April 1 snow water equivalent (SWE) to that of historical (1961-1990). 39

Abstract

Possible future climate changes in and their impacts in California are from a varied set of climate change model simulations. These simulations, conducted by three state-of-the-art global climate models, provide trajectories from three greenhouse gas (GHG) emission scenarios. These scenarios and the resulting climate simulations are not "predictions," but rather are a limited sample from among the many plausible pathways that may affect California's climate. Future GHG concentrations are uncertain because they depend on future social, political, and technological pathways, and thus the IPCC has produced four "families" of emission scenarios (IPCC, 2001). To explore some of these uncertainties, emissions scenarios A2 (a medium-high emissions) and B1 (low emissions) were selected from the current IPCC Fourth climate assessment, which provides several recent model simulations driven by A2 and B1 emissions. The global climate model simulations addressed here were from PCM1, the Parallel Climate Model from the NCAR and DOE group, and CM2.1 from the NOAA Geophysical Fluids Dynamics Laboratory (GFDL). For this study, a statistical technique using properties of historical weather data (Wood et al., 2002) was employed to correct model biases and "downscale" the global-model simulation of future climates to a finer level of detail, onto a grid of approximately 7 miles (12 kilometers), more suitable for impact studies at the scales needed by California decisionmakers.

In current climate-change simulations, temperatures over California warm significantly during the 21st century, with temperature increases from approximately +3ºF (1.5ºC) in the lower emissions scenario (B1) within the less responsive model (PCM1) to +8ºF (4.5ºC) in the higher emissions scenario (A2) within the more responsive model (CM2.1). Three of the simulations (all except the low emission scenario run of the low response model) exhibit more warming in summer than in winter. In all of the simulations, most precipitation continues to occur in winter, with virtually all derived from North Pacific winter storms. Relatively little change in overall precipitation is projected. Climate warming has a profound influence in diminishing snow accumulations, because there is more rain and less snow, and earlier snowmelt. These snow losses increase as the warming increases, so that they are most severe under climate changes projected by the more sensitive model with the higher GHG emissions.

1.0 Introduction

In May 2005, the California Energy Commission (Commission) and the California Environmental Protection Agency (Cal/EPA) commissioned a report describing the potential impacts of climate change on key state resources. It was recognized that current climate-change projections agree on certain broad and troubling aspects of the future climate and climate influences in 21st Century California. Despite considerable uncertainty in some key details (especially, regional details) of future climate change and a good measure of contrast between different global climate models, an up-to-date appraisal of potential impacts from the projections available would help to inform decisionmakers as they begin to address and plan for these impacts. Although precise prediction is impossible, it was agreed that it would be worthwhile to examine a selection of scenarios of possible climate change, targeted regionally to explore California's future climate, in a manner similar to previous and ongoing efforts by the Intergovernmental Panel on Climate Change (IPCC) (Houghton et al 2001), an examination of ecological and related changes in California (Field et al. 1999), the U.S. National Climate Change Assessment (National Assessment SynthesisTeam, 2001), and by scientists in Great Britain to examine potential climate changes in the United Kingdom (www.ukcip.org.uk/resources/publications/documents/UKCIP02_briefing.pdf). Because of the tight timeframe during which this work was to be completed, this assessment focuses on a small subset, namely two, of available global climate models.

A current effort by the international climate-science community to prepare the Fourth IPCC Climate Change Assessment provides important background and crucial inputs for the studies reported here. In particular, that international assessment has prompted and released a large number of climate model simulations using a selected set of the IPCC contrasting greenhouse gas (GHG) emission scenarios. Thus, the present effort has used only a few of the IPCC simulations to provide concrete examples of possible impacts and has used the larger ensembles of projections generated for the IPCC assessment to put those particular simulations into perspective and to explore, albeit in limited fashion, two major sources of climate-change uncertainty: our incomplete understanding of how the climate system responds (as represented by differences between different climate models) and the unknowable future of emissions of GHG and other manmade contaminants to the atmosphere (as represented by the GHG scenarios considered here). The purpose of this chapter is to describe the selection of the two climate models, properties of the two scenarios that were analyzed, how the global models were downscaled to the California region, and noteworthy properties of the model simulations of possible future climate change that are relevant to California impacts.

2.0 Climatological Characteristics in California: Observational Criteria

Criteria for model selection included realistic simulation of California regional climate—particularly the distribution of temperature and the strong seasonal cycle of precipitation that exists in this region. In addition, models selected should contain realistic large scale features, such as the spatial structure of precipitation. They should also include realistic variability at interdecadal and longer time scales during the

historical simulations, which should include tropical variability and associated teleconnections to extratropical variability (e.g. Dettinger et al. 2001), including those germane to California (Figures 1-3, and 7).

3.0 Natural Variability vs. Climate Forcing

In assessing climate change impacts, it is important to determine whether or not observed historical climate changes in California exceed the "noise" level of natural internal climate variability, as estimated from unforced climate model simulations.

This work is based upon previous climate change detection studies at global scales (e.g. Santer et al., 1996; Hegerl et al., 1997; North and Stevens, 1998; Tett et al., 1999;

Stott et al., 2000) and also in large regions (Stott, 2003; Zwiers and Zhang, 2003; Spagnoli et al., 2002; Karoly and Braganza, 2005), including North America (Karoly et al., 2003). We estimated the observed linear trend in surface temperature from the University of Washington monthly 1/8-degree gridded meteorological dataset (Maurer et al., 2002). We estimated the maximum possible trend due to natural climate variability (within a 90% confidence interval) from seven multi-century, unforced "control" simulations, by fitting linear trends to overlapping 50-year segments (following the approach of Karoly et al., 2003; Santer et al., 1995). These simulations are available in the context of the IPCC Fourth Assessment (AR4) and were performed using models that simulate a warming in California during the twentieth century: cccma_cgcm3_1, csiro_mk3_0, giss_aom, iap_fgoals1_0_g, and ipsl_cm4, gfdl cm2.1 and pcm 1.

The statewide-average annual-mean surface temperature increased by 0.57 deg K during 1949-1999 (Figure 4a and 4b). This warming slightly exceeds the limits of natural internal climate variability estimated from the unforced climate model simulations (with 90% level of confidence). This suggests the possibility that the observed trend is not entirely due to natural fluctuations of the atmosphere-ocean climate system alone, and therefore must be explained in part by the influence of external forcings. Because the observed warming over the last few decades shows a pronounced seasonality, with larger warming during winter and spring than during summer and fall (Figure 4a), this analysis was also conducted separately for each season (Figure 4b) . During summer and fall seasons, the observed warming trends are small and can be due to natural internal variability and/or a combination of counteracting external factors. On the other hand, during winter and spring, the observed warming trends during 1949-1999 were quite large in comparison to the natural internal variability contained in the model runs.

The results shown here suggest that the winter and spring warming that has occurred in the California region over the last few decades is very unlikely to have been caused only by natural climate variations. The implication is that some of this warming was the result of external influence(s), of either human (e.g. emission of greenhouses gases) or natural origin that have perturbed California's climate. The formal attribution of California's climate change to specific anthropogenic and natural forcings is however beyond the scope of this study.

4.0 Scenarios and Models Selected

Models were selected on the basis of the availability of climate model output data, the published track record of the modeling group, and representing different levels of sensitivity to GHG forcing (Figure 5). These criteria yielded two global climate models (GCMs), including PCM (Meehl and Washington group at NCAR in Boulder Colo., see Washington et al. 2000; Meehl et al. 2003) and GFDL CM2.1 (NOAA Geophysical Dynamics Laboratory, Princeton New Jersey; see Stouffer et al. 2005; Delworth et al. 2005; Knutson et al. 2005). GHG emissions scenarios A2 (medium-high emissions) and B1 (low emissions) choice was based upon decisions made by IPCC4 (Nakic'enovic' et al. 2000), and availability of relatively crucial output from model climate simulations. Scenario A1fi (high emissions) was used in the recent Hayhoe et al. (2004) study to assess implications of high and low GHG emissions scenarios and associated climate change impacts in California, and is included here because some of the related studies in this collective work report or compare those results. As shown in Figure 6, the B1 scenario has global (including California) CO_2 emissions peaking at approximately 10 gigatons per year (Gt/yr) in mid-century before dropping below current-day levels by 2100. [This corresponds to a doubling of CO_2 concentration relative to its pre-industrial level by the end of the century.] For the A2 scenario, CO_2 emissions continue to climb throughout the century, reaching almost 30 Gt/yr, so that by the end of the century CO_2 concentration reaches more than triple its pre-industrial level. The A1fi scenario has high emissions through about 2080 that level off from 2080 through 2100, and result in CO_2 concentrations that reach about 950ppm by 2100.

Both the GFDL and PCM groups performed historical simulations, the 20C3M experiments (see http://www-pcmdi.llnl.gov/projects/cmip/ann_20c3m.php) that allow us to compare global climate model performance to historical observations over late 19th and the entire 20th Centuries. 20C3M runs for GFDL cover 1861-2000 and for PCM cover 1890-1999. In the 20C3M simulations, both models account for historical estimates of inputs from volcanic eruptions, changes in solar irradiance, and anthropogenic GHG and aerosol loading (Delworth et al., 2005; Meehl et al., 2003). The 1961-1990 period of modeled climate is used in the present study as a climatology, a benchmark to compare recent modern climate with future climate projected by each of the models, respectively.

5.0 Characteristics of Model Simulations

Each of the model simulations contains symptoms of global climate change over the California region. As we know from previous studies, there is more consistency in the changes of some elements, such as temperature, than others, such as precipitation. Due to differences in the two models' sensitivities and responses to greenhouse gases and other forcings, there are substantial differences between the two models. PCM has relatively low sensitivity of global and regional temperature to GHG forcing and GFDL CM2.1 has relatively high sensitivity, as shown from a ranking of the increase in temperature change from a low emissions scenario B1 simulation to a medium-high emission scenario A2 simulation, charted for a larger set of IPCC models in Figure 5. Nonetheless, there are significant differences between the two GHG emission scenarios that grow over time, an aspect of this problem which has been emphasized in previous

studies (Hayhoe et al., 2004; IPCC, 2001.) and is again an important theme in the present results. Northern California temperature warms significantly between 2000 and 2100, from approximately 3ºF (1.5ºC) in the lower emissions scenario within the less responsive model to 8º (4.5C) in the higher emissions scenario within the more responsive model (see Table 1). To put this in perspective, these projected temperature changes over the next century are slightly larger than the difference in annual mean temperature between Monterey and Salinas, and between San Francisco and San Jose, respectively. The difference in annual mean temperatures between Monterey (65.3ºF) and Salinas (67.8ºF) is 2.5ºF and the difference between San Francisco Mission Delores (63.6ºF) and San Jose (71.0ºF) is 7.4ºF.

Regardless of which model is employed, the warming is greater for the higher emission scenario (SRES A2) than for the lower emission scenario (SRES B1). The rate of temperature increase over the 2000-2100 period is approximately linear in each of the four model runs, although there is substantial year to year variation. Additionally, from available A1fi simulations conducted in an earlier study by Hayhoe et al (2004) temperature changes were slightly higher than those for the A2 simulations examined here, judging from PCM simulations, which produce 6.8 ºF (3.8ºC) warming in A1Fi (Table 1 of Hayhoe et al 2004) and approximately 4.8 ºF (2.7ºC) warming in A2, as shown in Table 1.

In the first 30 year epoch, 2005-34, the change in temperature, even in the lower response model under the lower emissions scenario, amounts to an increase of summer and winter temperature by more than 0.5 C. This increase is sufficient to reduce(increase) substantially the number of cold(warm) temperature outbreaks in summer and winter temperature levels. By the last 30 year epoch considered, 2070-99, for each of the two scenarios considered here and the A1fi scenario analyzed by Hayhoe et al, 2004, effects of accumulated GHG emissions are greatest, increases in temperature are largest, and the resultant responses of other measures are largest. Over northern California, the summer temperature increase for the higher emissions scenario within the more responsive model is 11.6ºF (6.4ºC) while that for the lower emissions scenario is 6.6ºF (3.6ºC). Even in the lower response model under the lower emissions scenario, the temperature increases are sufficient to nearly eliminate seasonal mean temperatures falling into the lower third of the present historical distribution, and eliminate half or more of those expected in the middle third of the distribution, as provided by the counts of seasonal temperature values falling in the lower and middle tercile classes for Northern and Southern California model locations in Tables 2a and 2b, respectively.

An important aspect of the model results is that three of the simulations (all except the low emission scenario run of the low response model) yield more warming in summer than in winter. In the highest emission (A2) scenario for the PCM and GFDL simulations of mean temperature over northern California exhibit temperature increases by the end of the 21st century by 2.6ºC and 5.3ºC in summer and 2.4ºC and 3.3ºC in winter, respectively. If such a summer amplification of the projected warming trends, materializes, it has important implications for impacts such as ecosystems, agriculture, water and energy demand, and the occurrence of heat waves, which can have consequences for public health and the economy.

There is no indication from the projections that the Mediterranean seasonal precipitation regime in California will change, as indicated by the monthly mean precipitation for the B1 and A2 simulations of PCM and GFDL CM2.1 over northern California and southern California locations in Figure 8. In all of the simulations, most precipitation continues to occur in winter, with virtually all of it derived from North Pacific winter storms, as demonstrated by the correlations between Northern California monthly precipitation and 500HPa height (500millibar height), mapped over the Pacific and western North America domain in Figure 9 for the 2070-2099 period from the A2 simulations of GFDL and PCM in comparison to those from observations. Summer precipitation changes only incrementally, and actually decreases in some of the simulations, so there is no simulated indication of a stronger thunderstorm activity. Also, relatively small changes in overall precipitation are projected by the simulations, amounting to less than 20% and, usually, less than 10% change in any of the 4 projections. This is consistent with the fact that although, in general, under global warming, global rates of precipitation are projected to increase, these increases tend to be geographically focused in the tropics and higher latitude extra-tropics. In most current projections of global warming, subtropical and lower middle latitude regions exhibit little change in precipitation and in some cases become drier. In the present investigation, each of the model runs is characterized by large interannual to decadal fluctuations of precipitation, and modest changes, not consistently positive or negative, in annual precipitation during the 2000-2100 period. In Northern California, by end of century, projected precipitation increases slightly or does not change in one model (PCM), and decreases by 10- 20% in the other model (GFDL). Analysis of California precipitation changes produced under B1 and A2 emissions scenarios in 11 global climate models by Maurer (2005) also finds only modest changes in annual precipitation, but an increase in precipitation in winter months, but a decrease in spring months.

Moreover, little change in year-to-year variability of precipitation or temperature is evident in the model simulations as will be shown below from plots of ensembles of the same model and same scenario, simply run in perturbed fashion using different initial conditions. This relatively stationary in variability is important because large impacts often occur during anomalous years owing to floods, drought, heat waves, etc. The frequency of warm tropical events (El Niños) remains about the same as was exhibited in the historical simulations, and model El Niño events continue to be related to anomalous precipitation patterns over California.

To put the two scenarios and the two GCMs, that are the focus of this assessment into broader perspective, it is useful to compare them with projections of climate changes over California from a larger collection of simulations. Following an analysis by Dettinger (2005 and *in press*), projection distributions were estimated for a much larger subset of the Fourth IPCC Assessment simulations, including 84 simulations from a total of 12 different climate models responding to three different emission scenarios: higher (A1b), middle-high (A2), and low (B1). This larger ensemble of simulations describes a range of projected temperature changes, all positive, from relatively modest to quite large (from about +2°C to +7°C). The distribution of precipitation changes includes both positive and negative changes that cluster with little change around present-day averages (Figures 10 and 11). It can be seen from Figures10 and 11 and Table 1 that,

throughout the 100 year simulation, California conditions projected by PCM remain in the lower half of the temperature-change distributions, exhibiting a relatively modest degree of warming. The small changes experienced by PCM B1 and A2 are close to the center of the overall precipitation-change distributions. In contrast, Figure 10 and 11 show that California temperatures projected by GFDL and HadCM3 are in the warmer half of the overall temperature-change distributions. GFDL and HadCM3 projections of precipitation tend to be in the drier parts of the precipitation-change distributions. As discussed by Maurer (2005), when considering several of the recent model simulations, there is a tendency for precipitation to increase somewhat in winter months and to decrease in spring months.

Importantly, the statistical distributions of projections from the Fourth Assessment ensemble of models (from which the projections focused on here were drawn) are not qualitatively different from the corresponding distributions constructed from a smaller set of simulations that were contributed to the Third IPCC Assessment, published in 2001 (Dettinger, 2004). The Fourth Assessment projections of temperature changes yield about 0.85^{o}C less warming (overall) by end of 21st century than did the previous Third Assessment projections. Notably, the Fourth Assessment projections of precipitation changes do not include the influence of large projected increases in precipitation from the UK's HadCM2 or the Canadian CCCM models that appeared among the Third Assessment projections. Thus the resultant distributions are more consistently centered around historical values, as illustrated in Figures 9, 10a and 11. The overall similarities between the current projections and previous projections includes the PCM and GFDL models and B1 and A2 emission scenarios selected here, and indicate that results from many past climate-change studies continue to be informative and can usefully be compared to the present results. In the Fourth Assessment ensemble of projections considered here, both wetter *and* drier projections than today's precipitation levels have emerged from various of the warmest models, and likewise for the coolest models, as indicated by the model changes superimposed on the distributions of changes from recent IPCC simulations in Figures 10, 11 and the time series of projected temperature and precipitation changes from the present models vs the larger set of IPCC simulations in Figures 12a and 12b. Thus, the projected mean precipitation changes are not correlated with the projected mean temperature changes from a given model, as shown by the joint probability of temperature and precipitation changes in Figure 10.

An ensemble of simulations for historical conditions or for a given GHG emission scenario indicates the internal variability of a particular climate model. The intra-scenario variability for the two models is fairly high, as seen from a set of three ensembles of a) winter and b) summer temperature from the PCM A2 simulation in Figures 13a , and from a set of historical and climate change simulations of annual precipitation in Figure 13b. Despite this "natural model variability", the ensembles seem to reinforce the general character of the temperature warming, or alternatively, the varying but only incrementally changing volume of precipitation.

6.0 Bias Correction and Spatial Downscaling of GCM Output

The selection of GCMs to include in this study required that they exhibit, on a broad spatial scale, seasonal patterns of simulated precipitation and temperature for the

historic period that are plausible. However, even the best models display biases on regional scales that are large enough that the impacts of climate change to be difficult to establish. This problem has inspired the development of many different techniques for extracting the meaningful signals of future climate evolution from the raw GCM output while at the same time reproducing historical climate patterns on the landscape at local scales. Using consistent methods to process the data allows a comparison of both means and interannual variabilities in future periods to a historical period that reflects observed conditions. Many studies have used a shift or scaling factor derived by comparing a climate model's future precipitation or temperature to its climatology, applying this shift to a historical record (Lettenmaier and Gan, 1990; Miller et al., 2003). While this method effectively removes the bias of the mean GCM climatology from the future climate, it does not address the potential bias in the variability of the climate model and can constrain inter-annual variability to the historic observed levels.

Different methods of downscaling, to take the large scale signal from the GCM and translate it to the local scale, have been developed. This can be done with dynamical or statistical methods [see for example (Benestad, 2001; Mearns et al., 2001)]. The principal disadvantage of dynamic downscaling is that it requires intensive computational resources, which for the four 150-year transient simulations of this study would have been impossible, requiring months to years of computing time. For this study, we employed a statistical bias correction technique and downscaling technique originally developed by Wood et al. (2002) for using global model forecast output for long-range streamflow forecasting. This technique was later adopted to downscale GCM output for use in studies examining the hydrologic impacts of climate change (Hayhoe et al., 2004; Maurer and Duffy, 2005; Payne et al., 2004; Vanrheenen et al., 2004). This is an empirical statistical technique that maps precipitation and temperature during a historical period (1950–1999 for this study) from the GCM to the concurrent historical record, which for this study is taken to be a gridded National Climatic Data Center Cooperative Observer station data set (Maurer et al., 2002). This data set, developed at a spatial scale of 1/8° (about 7 miles (12km)), was aggregated to a 2° latitude-longitude spatial resolution.

The combined bias correction/spatial downscaling method used in this study has been shown to compare favorably to different statistical and dynamic downscaling techniques (Wood et al., 2004) in the context of hydrologic impact studies. For precipitation and temperature, cumulative distribution functions (CDFs) are built for each of 12 months for each of the 2° grid cells for both the gridded observations and each GCM (first interpolating raw GCM data onto a common 2° grid) for the historical period (1950–1999). GCM quantiles are then mapped onto the climatological CDF for the entire simulation period. For example, if precipitation at one grid point from the GCM has a value in January of 2050 equal to the median GCM value (for January) for 1950–1999, it is transformed to the median value of the January observations for 1950–1999. For temperature, the linear trend is removed prior to this bias correction step, and is replaced afterward, to avoid increasing sampling at the tails of the CDF as temperatures rise. Thus, the probability distributions of the observations are reproduced by the bias corrected climate model data for the overlapping historical period, while both the mean and variability of future climate can evolve according to GCM projections.

The GFDL model has a resolution (of the atmospheric component) of 2.5° longitude by 2.0° latitude (approximately 137 mi X 137 mi (220 km x 220 km) per grid cell), and the PCM uses a standard T42 resolution (approximately 2.8°, or 155 mi X 186 mi (250 km x 300 km) in California). A general idea of the spatial resolution of the GCMs can be seen from the temperature and precipitation maps in Figures 14 (right hand side) and 15 (top), respectively. As is clear, the spatial scale of the GCMs is very large compared to the scale of interest for many impact studies. For example, the area of one GCM atmospheric grid cell (simulated essentially as one area of constant elevation and land surface condition) is more than 10 times as large as the entire American River basin upstream of Folsom Dam. The Wood et al. (2002) statistical method interpolates the bias corrected GCM anomalies, expressed as a scale factor (for precipitation) and shift (for temperature) relative to the climatological period at each 2° GCM grid cell to the centers of 1/8 degree grid cells over California. These factors are then applied to the 1/8 degree gridded historical precipitation and temperature (see Figure 14, left hand side and Figure 15, lower.

7.0 Hydrologic Modeling

To generate supplemental meteorological forcing data (such as radiative forcing, humidity, etc.) as well as to derive land surface hydrological variables consistent with the downscaled forcing data, the variable infiltration capacity (VIC) model (Liang et al., 1994; Liang et al., 1996) was used. VIC is a macroscale, distributed, physically based hydrologic model that balances both surface energy and water over a grid mesh, and has been successfully applied at resolutions ranging from a fraction of a degree to several degrees latitude by longitude. The VIC model includes a "mosaic" land surface scheme, allowing a statistical representation of the sub-grid scale spatial variability in topography and vegetation/land cover. This is especially important when simulating the hydrologic response in complex terrain and in snow dominated regions. To account for subgrid variability in infiltration, the VIC model uses a scheme based on work by Zhao et al. (1980). The VIC model also features a nonlinear mechanism for simulating slow (baseflow) runoff response, and explicit treatment of a vegetation canopy on the surface energy balance. Following the simulation of the water and energy budgets by the VIC model, a second program is used to route the derived runoff through a defined river system to obtain streamflow at specified points. The algorithm used in this study, developed by Lohmann et al. (1996), has since its development been employed in all simulations of streamflow using output from the VIC model. The VIC model has been successfully applied in many settings, from global to river basin scale (Abdulla et al., 1996; Maurer et al., 2001; Maurer et al., 2002; Nijssen et al., 1997; Nijssen et al., 2001), as well as in several studies of hydrologic impacts of climate change (Christensen et al., 2004; Hayhoe et al., 2004; Maurer and Duffy, 2005; Payne et al., 2004; Wood et al., 2004). For this study, the model was run at a 1/8-degree resolution (measuring about 150 km^2 per grid cell) over the entire California domain, including all land surface area between latitudes 32°N and 44°N and west of longitude 113°W. For deriving streamflows within the Sacramento-San Joaquin river basin the identical parameterization to VanRheenen et al. (2004) was used.

Although precipitation changes only modestly over the period of the climate simulation, climate warming is projected to reduce snow accumulation in California. This is because warming causes more of the precipitation to fall as rain and less as snow (Knowles et al. 2005). Such changes in precipitation form (more rain and less snow) are indicated by substantial changes in daily temperature during days with precipitation, shown in Figure 16 for Northern California from the GFDL model. Notably, minimum temperatures tend to be warmest during days with the heaviest precipitation. For each model and each emission scenario, all precipitation categories, including dry days, exhibit a shift to warmer temperatures in the 2070-99 period relative to the historical climatological distribution.

During the historical period, snow accumulation has already shown losses of order 10% of April 1 snow water equivalent (SWE) across the western conterminous United States (Mote et al 2005), and is expected to melt earlier as climate warming continues (Knowles and Cayan 2002; Wood et al. 2004; Maurer and Duffy 2005). Each of the climate simulations, when used as input to the VIC hydrologic model, yields substantial losses of spring snow accumulation over the Sierra Nevada mountains. These losses become progressively larger as warming increases during the course of the 21st Century. The losses are also largest by end of century in projected responses to the simulated climates from the more sensitive model under the higher GHG emissions. As depicted in Table 3, and Figures 17, 18 and 19, the losses (negative) or gains (positive) of April 1 snow water equivalent (SWE) in the San Joaquin, Sacramento and Trinity drainages, as percentages of (1961-1990) historical averages, range from +6% to -29% (for the 2005-2034 period), from -12% to -42% (for 2035-64), and from -32% to -79% (for the 2070-99 period). The GFDL model, with its greater temperature sensitivity to increased GHG concentrations, produces snowpack losses about twice as large as those produced by the PCM. Most but not all of this difference can be ascribed directly to the projected warmings. However, the amounts of snowfall, and thus snowpack, also vary from model to model because 21st Century precipitation in the PCM simulations ranges from slightly wetter to about the same as historical levels whereas the GFDL simulations become somewhat drier than historical levels. For both models, snowpack losses are greatest in the warmer, more GHG-emitting (A1) scenario. By 2070-2099, virtually no snow is left below 1000m under this scenario. In terms of water storage volume, snow losses have greatest impact in relatively warm low-middle and middle elevations between about 3280 feet (1000m) and 6560 feet (2000m) , with losses of 60% to 93% and between about 6560 feet (2000m) and 9840 feet (3000m), with losses of 25% to 79%. Because the higher elevations of the Sierra Nevada are skewed to the southern portion of the range, the heaviest reductions in snow accumulation will occur in the central and northern portions of the mountain range (Figure 19).

8.0 References

http://nomads.gfdl.noaa.gov/CM2.X/

Abdulla, F. A., D. P. Lettenmaier, E. F. Wood, and J. A. Smith, 1996: Application of a macroscale hydrologic model to estimate the water balance of the Arkansas-Red River basin. *J. Geophysical Research*, ***101***, 7449-7459.

Benestad, R. E., 2001: A comparison between two empirical downscaling strategies. *Intl J. Climatology*, ***21***, 1645-1668.

Christensen, N. S., A. W. Wood, N. Voisin, D. P. Lettenmaier, and R. N. Palmer, 2004: The effects of climate change on the hydrology and water resources of the Colorado River basin. *Climatic Change*, ***62***, 337-363.

Delworth, T. et al., 2005: GFDL's CM2 global coupled climate models - Part 1: Formulation and simulation characteristics. *J. Climate*, April 2005, *(accepted for publication).*

Dettinger, M.D., 2005: From climate-change spaghetti to climate-change distributions for 21st Century California. San Francisco Estuary and Watershed Science, **3**(1), http://repositories.cdlib.org/jmie/sfews/vol3/iss1/art4 .

Dettinger, M.D., 2005: A component-resampling approach for estimating probability distributions from small forecast ensembles. Climatic Change, 31 p. (*in press*).

Dettinger, M.D., Battisti, D.S., Garreaud, R.D., McCabe, G.J., and Bitz, C.M., 2001: *Interhemispheric effects of interannual and decadal ENSO-like climate variations on the Americas*, in V. Markgraf (ed.), Interhemispheric climate linkages: Present and Past Climates in the Americas and their Societal Effects. Academic Press, 1-16.

Field, C. B., Daily, G. C., Davis, F. W., Gaines, S., Matson, P. A., Melack, J. & Miller, N. L. , 1999: *Confronting Climate Change in California: Ecological Impacts on the Golden State.* Union of Concerned Scientists, Cambridge, MA, and Ecological Society of America, Washington, DC.

Hanemann, L. S. Kalkstein, J. Lenihan, C. K. Lunch, R. P. Neilson, S. C. Sheridan, and J. H. Verville, 2004: Emissions pathways, climate change, and impacts on California. *Proceedings of the National Academy of Sciences of the United States of America*, **101**, 12422-12427.

Hayhoe, K., D. Cayan, C. B. Field, P. C. Frumhoff, E. P. Maurer, N. L. Miller, S. C. Moser, S. H. Schneider, K. N. Cahill, E. E. Cleland, L. Dale, R. Drapek, R. M. ,2004: Emissions pathways, climate change, and impacts on California. PNAS **101**(34):12422-12427, 24 August 2004.

Hegerl, G.C., H. von Storch, K. Hasselmann, B.D. Santer, U. Cubasch, P.D. Jones, 1996: Detecting Greenhouse-Gas-Induced Climate Change with an Optimal Fingerprint Method. *J. Climate* **9**(10), 2281-2306.

Hegerl, G.C., K. Hasselmann, U. Cubasch, J.F.B. Mithchell, E. Roeckner, R. Voss nd J. Waszkewitz, 1997: Multi-fingerprint detection and attribution analysis of Green house gas, greenhouse gas-plus-aerosol, and solar forced climate change. Clim. Dyn. **13**, 613-634.

Houghton, J. T., et al., (eds.), 2001: *The scientific basis: Contribution of Working Group I to the Third Assessment Report of the Intergovernmental Panel on Climate Change.* Climate Change, Cambridge University Press, 525–582.

Karoly, D.J. and K. Braganza, 2005: A new approach to detection of anthropogenic temperature changes in the Australian region. *Meteorol. Atmos. Phys,* **89**, 57-67.

Karoly, D.J., 2003: *Detection of anthropogenic climate change in the North American region.* AMS 14th Global Change Symposium, Long Beach, California, 9-13 Feb. 2003.

Karoly,D.J., K. Braganza, P.A. Stott, J.M. Arblaster, G.A. Meehl, A.J. Broccoli and K.W. Dixon, 2003: Detection of a human influence on North American climate. Science **302**, 1200-1203.

Knowles, N. & Cayan, D. R., 2002: Potential effects of global warming on the Sacramento/San Joaquin watershed and the San Francisco estuary. *Geophys. Res. Lett.* **29**(18)**,** 1891–1895.

Knowles, N., M.D. Dettinger and D.R. Cayan, 2005: Trends in Snowfall versus Rainfall in the Western United States. *J. Climate*, in review.

Knutson, et al., 2005: Assessment of Twentieth Century Regional Surface Temperature Trends using the GFDL CM2 Coupled Models. *J. Climate,* Sept. 2005, (*accepted*).

Lettenmaier, D. P., and T. Y. Gan, 1990: Hydrologic Sensitivities of the Sacramento-San Joaquin River Basin, California, to Global Warming, edited. Water Resources Research, pp. 69-86.

Liang, X., D. P. Lettenmaier, E. Wood, and S. J. Burges, 1994: A simple hydrologically based model of land surface water and energy fluxes for general circulation models. *J. Geophysical Research*, **99**(D7), 14,415-414, 428.

Liang, X., D. P. Lettenmaier, and E. F. Wood, 1996: One-dimensional statistical dynamic representation of subgrid spatial variability of precipitation in the two-layer variable infiltration capacity model. *J. Geophysical Research*, **101**(D16), 21, 403-421, 422.

Lohmann, D., R. Nolte-Holube, and E. Raschke, 1996: A large-scale horizontal routing model to be coupled to land surface parameterization schemes. *Tellus*, **48A**, 708-721.

Maurer, E.P., 2005, Uncertainty in hydrologic impacts of climate change in the Sierra Nevada Mountains, California under two emissions scenarios, *Climatic Change* (in review).

Maurer, E. P., and P. B. Duffy, 2005: Uncertainty in projections of streamflow changes due to climate change in California, *Geophysical Research Letters*, **32**, L03704.

Maurer, E. P., A. W. Wood, J. C. Adam, D. P. Lettenmaier, and B. Nijssen, 2002: A Long-Term Hydrologically-Based Data Set of Land Surface Fluxes and States for the Conterminous United States. *J. Climate*, **15**(22), 3237-3251.

Maurer, E. P., G. M. O'Donnell, D. P. Lettenmaier, and J. O. Roads, 2001: Evaluation of the land surface water budget in NCEP/NCAR and NCEP/DOE reanalyses using an off-line hydrologic model. *J. Geophysical Research*, **106**(D16), 17841-17862.

Mearns, L. O., M. Hulme, T. R. Carter, R. Leemans, M. Lal, and P. Whetton, 2001: *Climate scenario development*, in Climate Change 2001: The Scientific Basis, edited by J. T. e. a. Houghton, pp. 739-768, Cambridge University Press, New York.

Meehl, G.A., W.M. Washington, T.M.L. Wigley, J.M. Arblaster and A. Dai, 2003: Solar and Greenhouse Gas Forcing and Climate Response in the Twentieth Century. *J. Climate*, **16**(3), 426-444.

Miller, N. L., K. E. Bashford, and E. Strem, 2003: Potential impacts of climate change on California hydrology. *J. the American Water Resources Association*, **39**, 771-784.

Mote, Philip W., Hamlet, Alan F., Clark, Martyn P., Lettenmaier, Dennis P. Declining mountain snowpack in western North America, 2005:. *Bulletin of the American Meteorological Society*, **86**, 39-49

National Assessment Synthesis Team, 2001: Climate Change Impacts on the United States: *The Potential Consequences of Climate Variability and Change*, US Global Change Research Program**.**

Nakic´enovic´, N., J. Alcamo, G. Davis, B. de Vries, J. Fenhann, S. Gaffin, K. Gregory, A. Gru¨bler, T. Y. Jung, T. Kram, *et al.,* 2000: *Intergovernmental Panel on Climate Change Special Report on Emissions Scenarios.* Cambridge Univ. Press, Cambridge, U.K.

Nijssen, B., D. P. Lettenmaier, X. Liang, S. W. Wetzel, and E. Wood, 1997: Streamflow simulation for continental-scale basins, *Water Resources Research*, **33**, 711-724.

Nijssen, B., G. M. O'Donnell, D. P. Lettenmaier, D. Lohmann, and E. F. Wood, 2001: Predicting the discharge of global rivers. *J. Climate*, **14**(15), 1790-1808.

North G.R. and M.J. Stevens, 1998: Detecting climate signals in the surface temperature record, *J. Climate*, **11**(4), 563-577.

Payne, J. T., A. W. Wood, A. F. Hamlet, R. N. Palmer, and D. P. Lettenmaier, 2004: Mitigating the effects of climate change on the water resources of the Columbia River Basin. *Climatic Change,* **62***,* 233-256.

Santer, B. D., T.M.L Wigley, T.P. Barnett, E. Anyamba, 1996: Detection of climate change and attribution of causes. Cambridge University Press, New York, NY (USA).

Santer B.D., U. Mikolajewicz, W. Bruggemann, U. Cubasch, K. Hasselmann, H. Hock, E. Maierreimer, T.M.L. Wigley, 1995: Ocean variability and its influence on the detectability of greenhouse warming signals. *J. Geophys. Res. Oceans,* **100**(C6), 10693-10725.

Spagnoli B., S. Planton, M. Deque, O. Mestre and J.-M. Moisselin, 2002: Detecting climate change at a regional scale: The case of France. *Geophys. Res. Let.,* **29**(10) (DOI:10.1029/2001GL014619).

Stouffer et al, 2005: GFDL's CM2 global coupled climate models - Part 4: Idealized climate response. *J. Climate, (accepted for publication).*

Stott P.A., 2003: Attribution of regional-scale temperature changes to anthropogenic and natural causes. *Geophys. Res. Let.*, **30**(14).

Stott P.A., S.F.B. Tett, G.S. Jones, M.R. Allen, J.F.B. Mitchell and G.J. Jenkins, 2000: External control of 20th century temperature by natural and anthropogenic forcings. Science, **290**, 2133-2137.

Tett, S. F. B., P. A. Stott, M. R. Allen, W. J. Ingram, and J. F.B. Mitchell, 1999: Causes of twentieth century temperature change. *Nature*, **399**, 569-572.

Vanrheenen, N. T., A. W. Wood, R. N. Palmer, and D. P. Lettenmaier, 2004: Potential implications of PCM climate change scenarios for Sacramento-San Joaquin River Basin hydrology and water resources. *Climatic Change*, **62**, 257-281.

Washington, W. M., Weatherly, J. W., Meehl, G. A., Semtner, A. J., Bettge, T. W., Craig, A. P., Strand, W. G., Arblaster, J., Wayland, V. B., James, R. & Zhang, Y., 2000: *Clim. Dyn.* **16**(10/11), 755–774.

Wood, A. W., L. R. Leung, V. Sridhar, and D. P. Lettenmaier, 2004: Hydrologic implications of dynamical and statistical approaches to downscaling climate model outputs. *Climatic Change*, **62**, 189-216.

Wood, A. W., E. P. Maurer, A. Kumar, and D. P. Lettenmaier, 2002: Long-range experimental hydrologic forecasting for the eastern United States, *J. Geophysical Research-Atmospheres*, **107**(D20), 4429.

Zhao, R.-J., L.-R. Fang, X.-R. Liu, and Q.-S. Zhang, 1980: The Xinanjiang model, in *Hydrological Forecasting, Proceedings, Oxford Symposium*, edited, pp. 351-356, IAHS Publ. 129.

Zwiers, F.W., and X. Zhang, 2003: Toward Regional-Scale Climate Change Detection *J. Climate,* **16**(5), 793-797.

Table 1. Temperature and Precipitation Changes, GFDL and PCM B1 and A2 simulations, Northern and Southern California. Temperature units are ºC, precipitation in mm. Mean values are provided for historical (1961-1990) period, and changes between successive 30year periods are shown in subsequent columns for the models/emission scenarios, as indicated.

					2005-2034				2035-2064				2070-2099			
	Change in Statewide AVG Temps	units	1961-1990		GFDL		PCM		GFDL		PCM		GFDL		PCM	
			GFDL	PCM	A2	B1	A2	B1	A2	B1	A2	B1	A2	B1	A2	B1
NOCAL	Annual	°C	9.3	8.0	1.5	1.4	0.5	0.5	2.3	2.2	1.3	.8	4.5	2.7	2.6	1.5
	Summer(JJA)	°C	21.5	17.9	2.1	1.7	0.9	0.6	3.4	2.6	1.7	1.1	6.4	3.7	3.3	1.6
	Winter(DJF)	°C	-.46	.08	1.4	1.3	0.1	0.7	1.7	2.1	0.9	2.4	3.4	2.3	2.3	1.7
	Annual	mm/%	1098	750	+0.3	+2.0	-0.4	+6.8	-3.0	-1.9	-2.0	+2.8	-17.5	-9.3	-2.4	0.0
	Summer(JJA)	mm/%	13.7	13.7	-29.2	-5.8	+27.7	+43.8	-67.2	-13.1	+35.1	-17.5	-67.9	-43.1	-29.9	-3.6
	Winter(DJF)	mm/%	648.7	386.1	-1.3	+12.9	-5.0	+13.3	+6.2	-0.1	-5.0	-2.0	-9.1	-5.6	+4.3	+4.4

					2005-2034				2035-2064				2070-2099			
	Change in Statewide AVG Temps	units	1961-2000		GFDL		PCM		GFDL		PCM		GFDL		PCM	
			GFDL	PCM	A2	B1	A2	B1	A2	B1	A2	B1	A2	B1	A2	B1
SOCAL	Annual	°C	12.2	14.3	1.3	1.3	0.5	0.6	2.3	2.1	1.2	0.8	4.4	2.7	2.5	1.6
	Summer(JJA)	°C	23.2	23.4	1.7	1.6	0.4	0.5	3.1	2.3	1.3	0.8	5.3	3.2	2.6	1.5
	Winter(DJF)	°C	2.4	5.4	1.0	1.0	0.2	0.7	1.7	1.6	1.0	0.6	3.3	2.0	2.4	1.6
	Annual	mm/%	537	342	-6.1	-1.7	+7.0	+17.5	-1.7	-11.2	+7.0	-1.8	-26.3	-21.8	+7.9	+7.0
	Summer(JJA)	mm/%	7.2	5.4	+48.7	-12.5	-7.4	+5.6	-59.7	-50.0	+35.2	+33.3	-44.4	-62.5	-11.1	+1.9
	Winter(DJF)	mm/%	320.3	186.7	-0.7	+0.8	+1.1	+31.9	+8.7	-8.6	+6.3	-6.1	-1.7	-25.7	+8.4	-0.8

Table 2a. Seasonal temperature occurrences in historical tercile classes, Northern California. Temperature units are ºCelsius. σ is standard deviation, μ is mean, T1 and T2 are lower and upper tercile thresholds of (1961-1990) historical distribution, n1 is median, N1 is number of seasons within period whose mean temperature falls into lower tercile of (1961-1990) distribution; N1+N2 is number falling into lower and middle terciles of (1961-1990) distribution.

		Historical					2005-2034			2035-2064			2070-2099		
	Model Scenario Months	σ	μ	T1	T2	n1	N1	N1+N2	n1	N1	N1+N2	n1	N1	N1+N2	n1
NOCAL	GFDL A2 *DJF*	1.486	-.456	-.95	.5	-.098	0	11	6	4	9	5	0	3	1
	GFDL A2 *JJA*	1.234	21.58	20.99	22.14	21.67	0	5	4	0	0	0	0	0	0
	GFDL B1 *DJF*	1.486	-.456	-.95	.5	-.098	2	13	9	1	4	2	1	5	3
	GFDL B1 *JJA*	1.234	21.58	20.99	22.14	21.67	0	2	0	0	2	1	0	0	0
	PCM A2 *DJF*	1.921	.0868	-.52	1.17	.546	10	22	17	2	18	11	0	7	2
	PCM A2 *JJA*	0.901	17.96	17.59	18.42	17.89	1	8	4	1	1	1	0	0	0
	PCM B1 *DJF*	1.921	.0868	-.52	1.17	.546	4	19	9	7	20	15	0	9	3
	PCM B1 *JJA*	0.901	17.96	17.59	18.42	17.89	5	12	8	1	7	3	2	4	3

Table 2b. Seasonal temperature occurrences in historical tercile classes, Southern California. Temperature units are ºCelsius. σ is standard deviation, μ is mean, T1 and T2 are lower and upper tercile thresholds of (1961-1990) historical distribution, n1 is median, N1 is number of seasons within period whose mean temperature falls into lower tercile of (1961-1990) distribution; N1+N2 is number falling into lower and middle terciles of (1961-1990) distribution.

		Historical					2005-2034			2035-2064			2070-2099		
	Model Scenario Months	σ	μ	T1	T2	n1	N1	N1+N2	n1	N1	N1+N2	n1	N1	N1+N2	n1
SOCAL	GFDL A2 *DJF*	1.227	2.48	1.93	3.24	2.51	1	13	5	2	5	4	0	1	0
	GFDL A2 *JJA*	1.202	23.20	22.79	24.01	23.14	1	3	2	0	0	0	0	0	0
	GFDL B1 *DJF*	1.227	2.48	1.93	3.24	2.51	2	12	8	1	7	3	1	4	1
	GFDL B1 *JJA*	1.202	23.20	22.79	24.01	23.14	0	4	1	0	2	0	0	0	0
	PCM A2 *DJF*	1.416	5.45	4.71	6.27	5.83	7	18	14	2	11	5	0	2	0
	PCM A2 *JJA*	1.043	23.58	22.96	24.01	23.58	3	13	11	1	4	3	0	0	0
	PCM B1 *DJF*	1.416	5.45	4.71	6.27	5.83	2	15	5	4	17	11	0	4	3
	PCM B1 *JJA*	1.043	23.58	22.96	24.01	23.58	4	19	11	1	11	4	0	4	2

Table 3. Change in April 1 snow accumulation, San Joaquin, Sacramento, and parts of Trinity drainages from VIC hydrologic model. Similar computations for HadCM3 A1fi and B1 simulations and for PCM A1fi simulation are presented in Table 1 of Hayhoe et al., 2004.

			2005-2034				2035-2064				2070-2099			
Change in April snowpack SWE	Units	1961-1990	PCM		GFDL		PCM		GFDL		PCM		GFDL	
		PCM	B1	A2	B1	A2	B1	A2	B1	A2	B1	A2	B1	A2
1000-2000 m elevation	%	4.0 km^3	-.13	-.35	-.2	-.48	-.26	-.52	-.68	-.61	-.60	-.76	-.75	-.93
2000-3000 m elevation	%	6.5 km^3	+.12	-.09	-.04	-.33	-.08	-.21	-.36	-.32	-.25	-.34	-.56	-.79
3000-4000 m elevation	%	2.49 km^3	+.19	+.01	+.04	-.13	-.02	-.05	-.16	-.11	-.05	-.02	-..41	-.55
All elevations	%	13.0 km^3	+.06	-.15	-.07	-.29	-.12	-.27	-.42	-.37	-.32	-.41	-.59	-.79

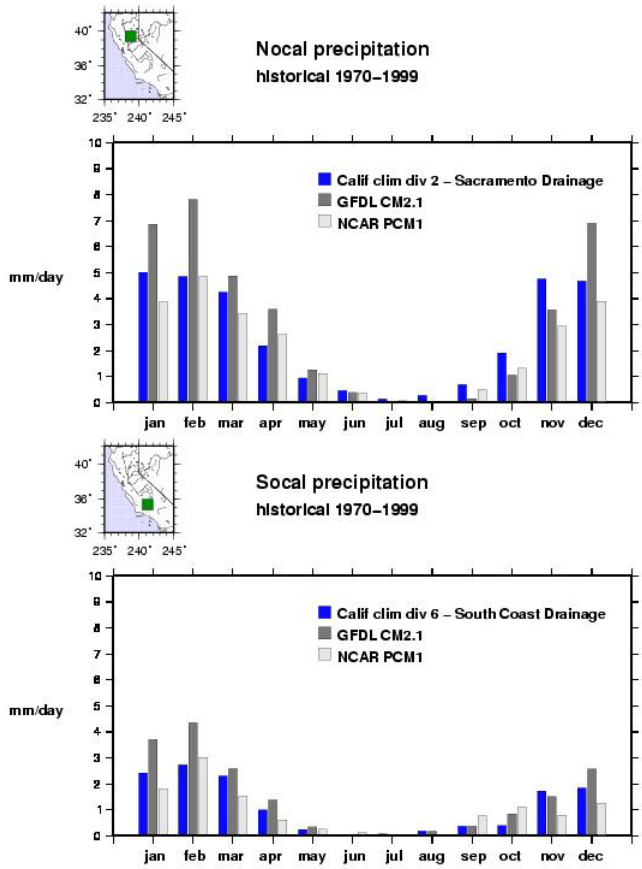

Figure 1. Observed and modeled precipitation, Northern and Southern California

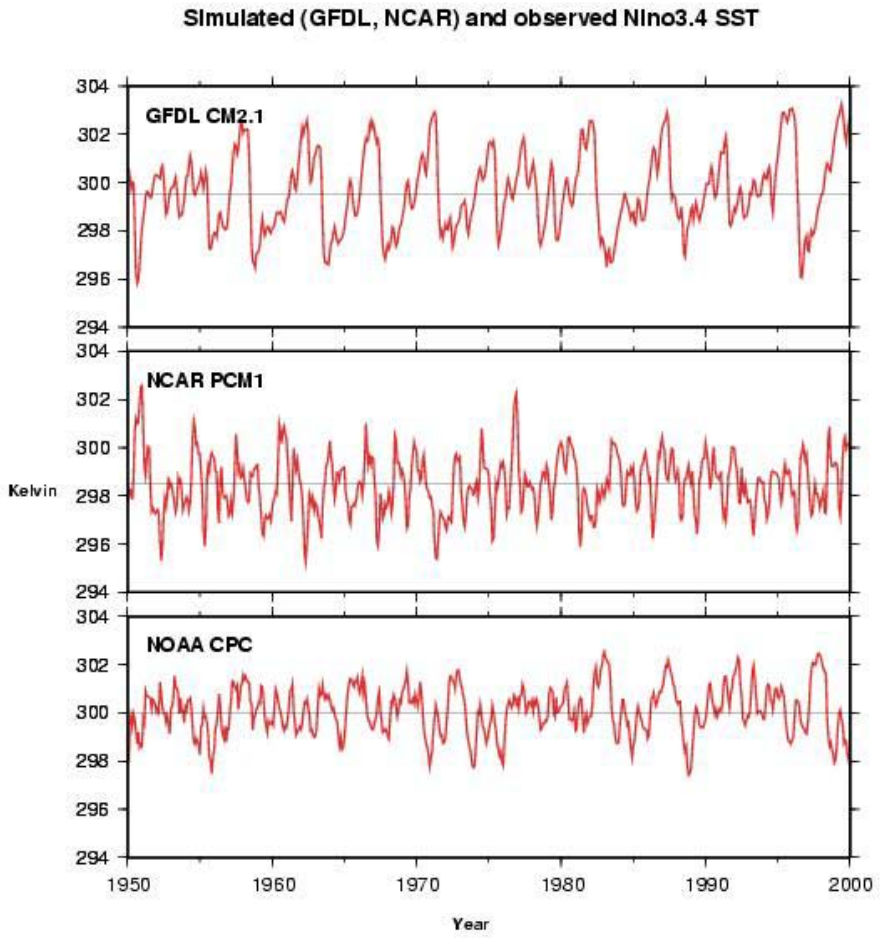

Figure 2. Tropical Pacific sea surface temperature (SST), Nino 3.4 region, GFDL and PCM historical simulations, and NOAA CPC observations, 1950-2000.

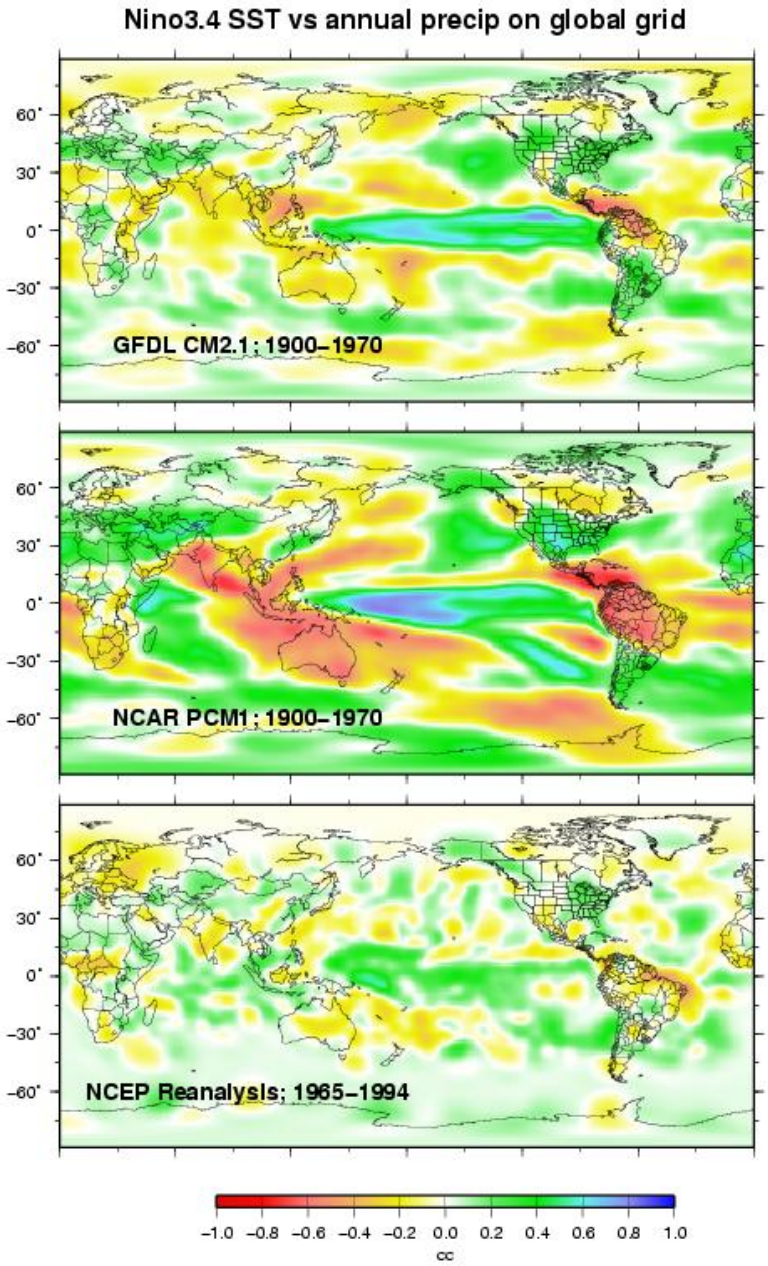

Figure 3. Correlation between Nino 3.4 SST and precipitation across the globe from simulations GFDL (above) and PCM (middle), along with observations from NCEP/NCAR Reanalysis www.cdc.noaa.gov/cdc/reanalysis/reanalysis.shtml (below) demonstrate reasonably strong connection between tropical Pacific ENSO fluctuations and extratropical precipitation.

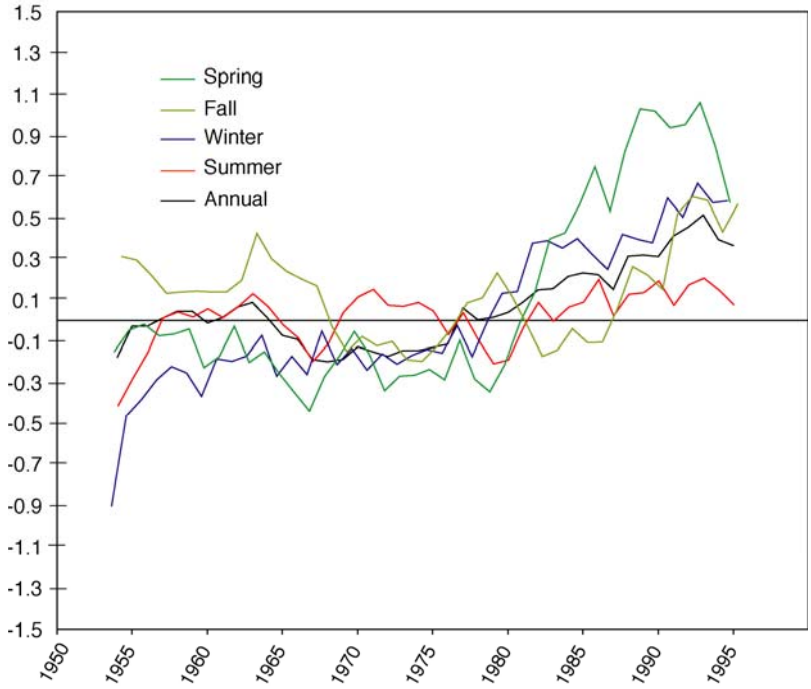

Figure 4a. 10-year running average of temperature anomalies (deg C) for California relative to the 1961-1990 base period average using annual (black), winter (blue),spring (green), summer (red), fall (brown) means. The time-series are computed from the UW monthly 1/8-degree gridded meterological dataset.

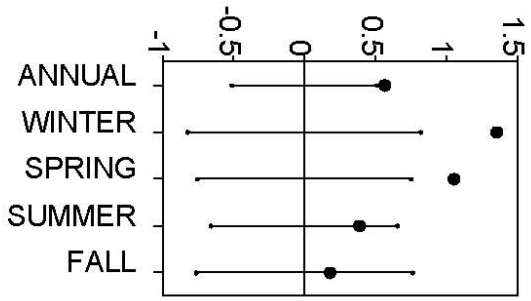

Figure 4b. Estimated natural variability of California temperature without forcing (bars), and observed temperature change (dots) during the 1950-2000 historical record.

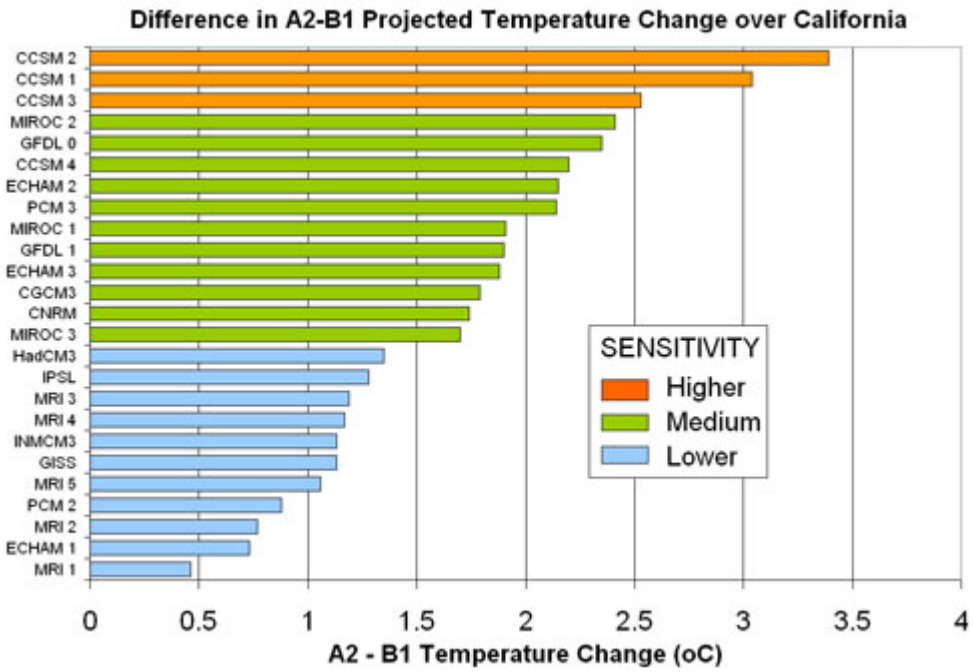

Figure 5. Climate sensitivity as gaged by difference in simulated gobal temperature over California. There are two runs each for GFDL (GFDL 0 and GFDL 1), and PCM (PCM2 and PCM3).

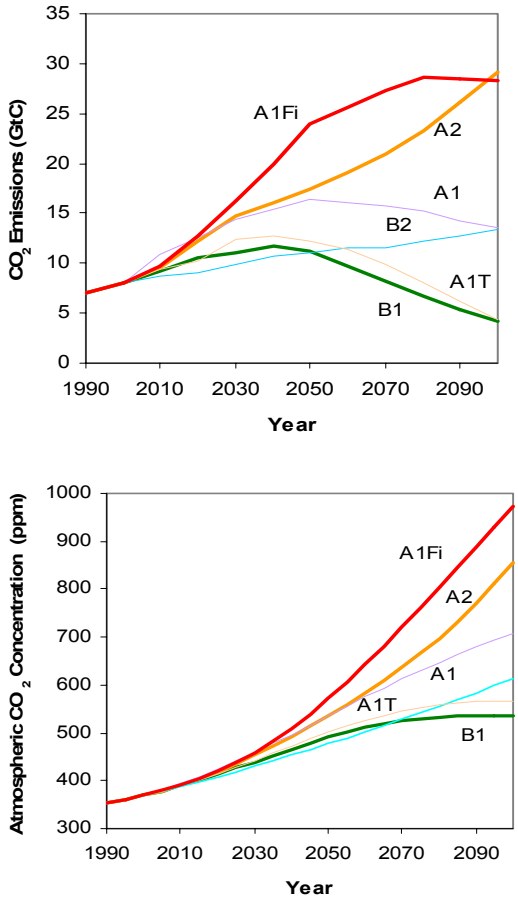

Figure 6. GHG (CO_2) emissions (above) and atmospheric concentrations (below) prescribed by IPCC for several emissions scenarios, including B1, A2 and A1Fi.

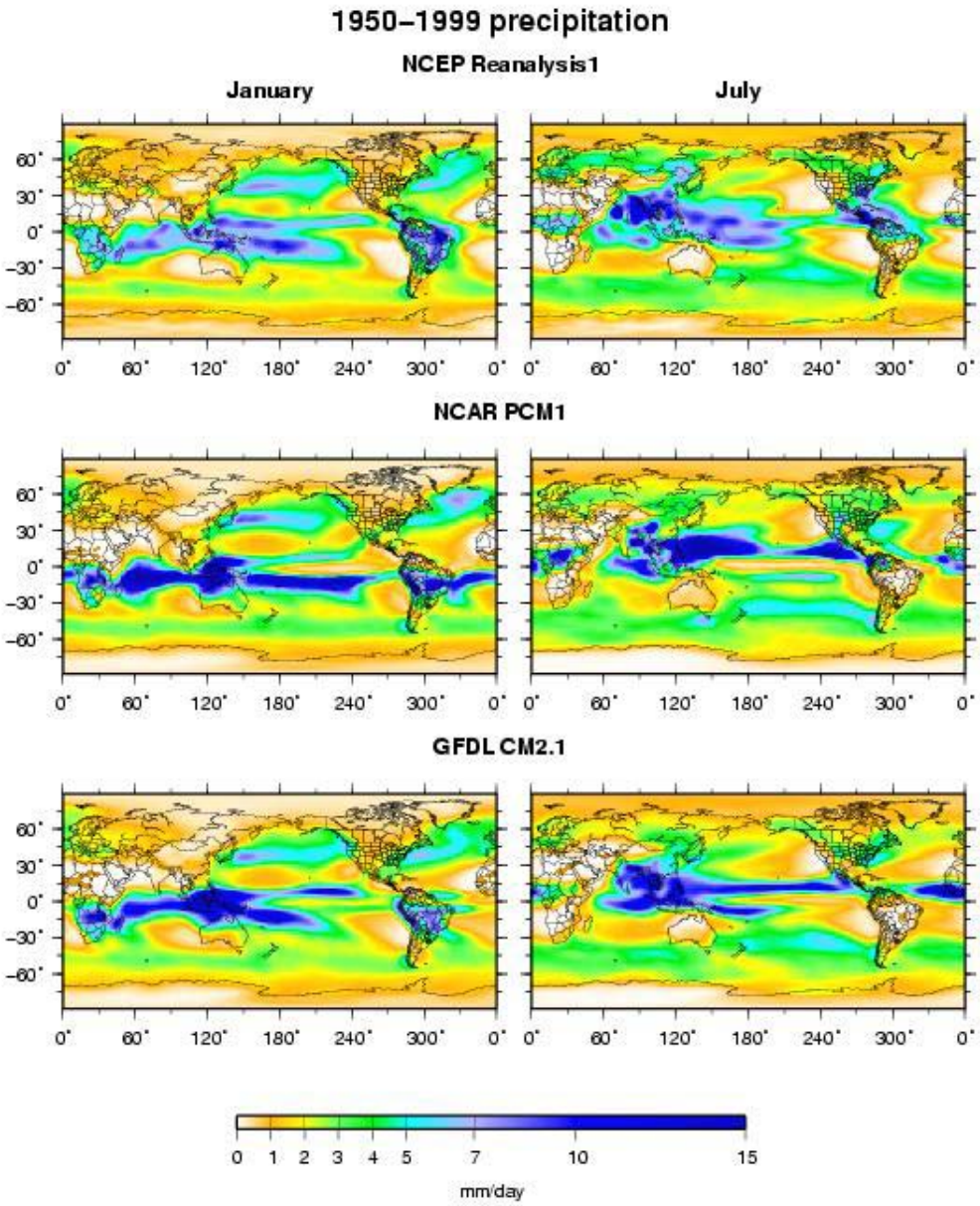

Figure 7. Global precipitation for January and July from Reanalysis (model version of observations), PCM, and GFDL historical model runs

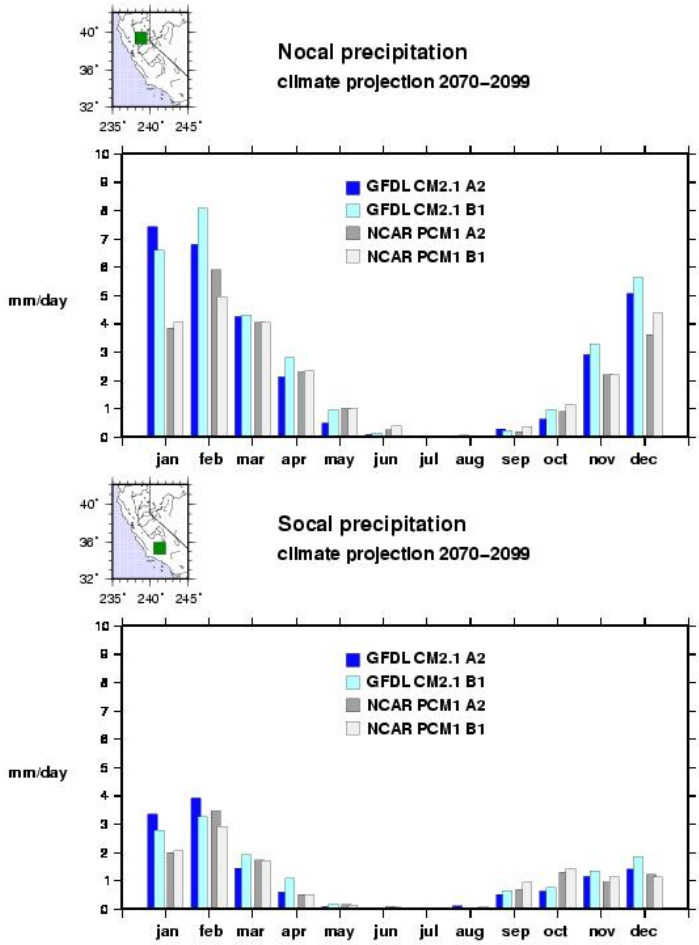

Figure 8. Projected Precipitation 2070-2099, Northern and Southern California. Compare with GCM historical and observed precipitation in Figure 1.

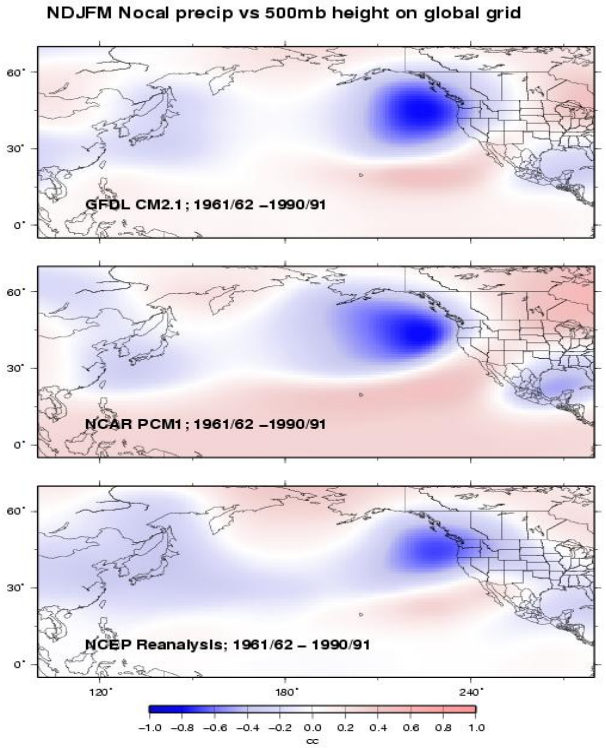

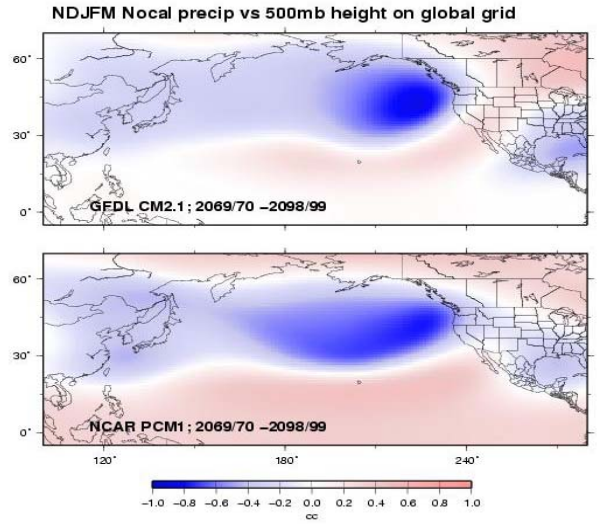

Figure 9. Correlations between Nov-Mar mean precipitation, Northern California, and Nov-Mar 500HPa height anomalies at each point in Pacific-western North America domain for (1961-1990) historical period and for 2070-2099 of GFDL and PCM A2 simulations, and for observations from NCAR/NCEP Reanalysis.

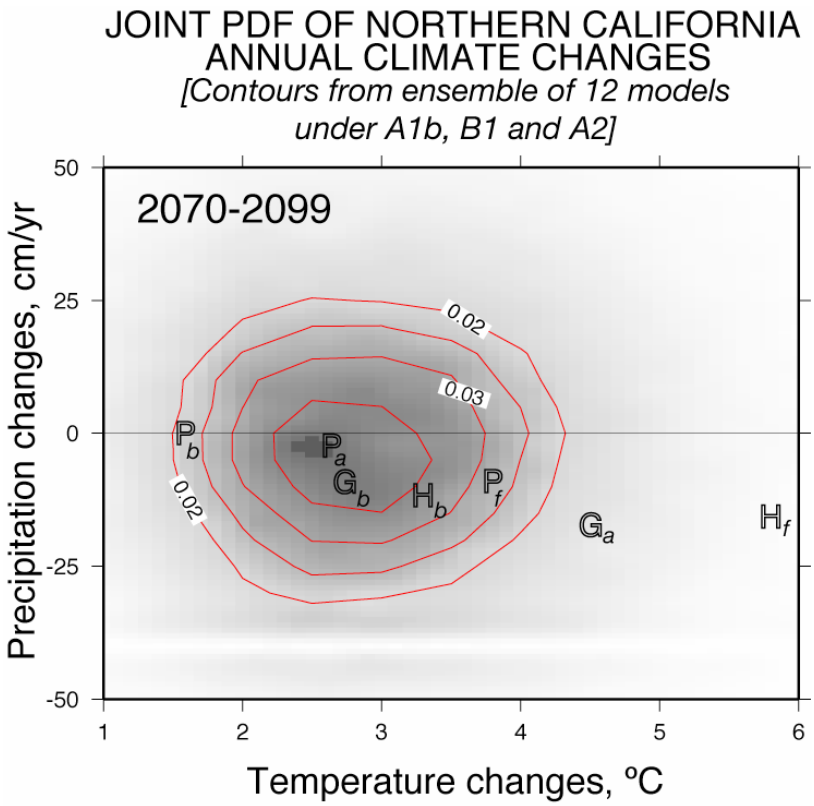

Figure 10. Joint Probability Distribution, Temperature and Precipitation Change 2070-2099, constructed from ensemble of IPCC AR4 model simulations. This shows, from a sampling of a collective of three different emissions scenarios run by 13 different global climate models, the probability of a given pairing of changes of temperature and precipitation in 2070-2099 relative to their historical means during 1961-1990. Isopleths define loci of points having equal probability, as labeled. Superimposed upon the matrix of joint probablilities are specific results considered in the present Scenarios Project: GFDL CM2.1 (G), PCM (P), and HadCM3 (H) models, under emission scenarios B1 (b), A2 (a), and A1fi (f) are labeled.

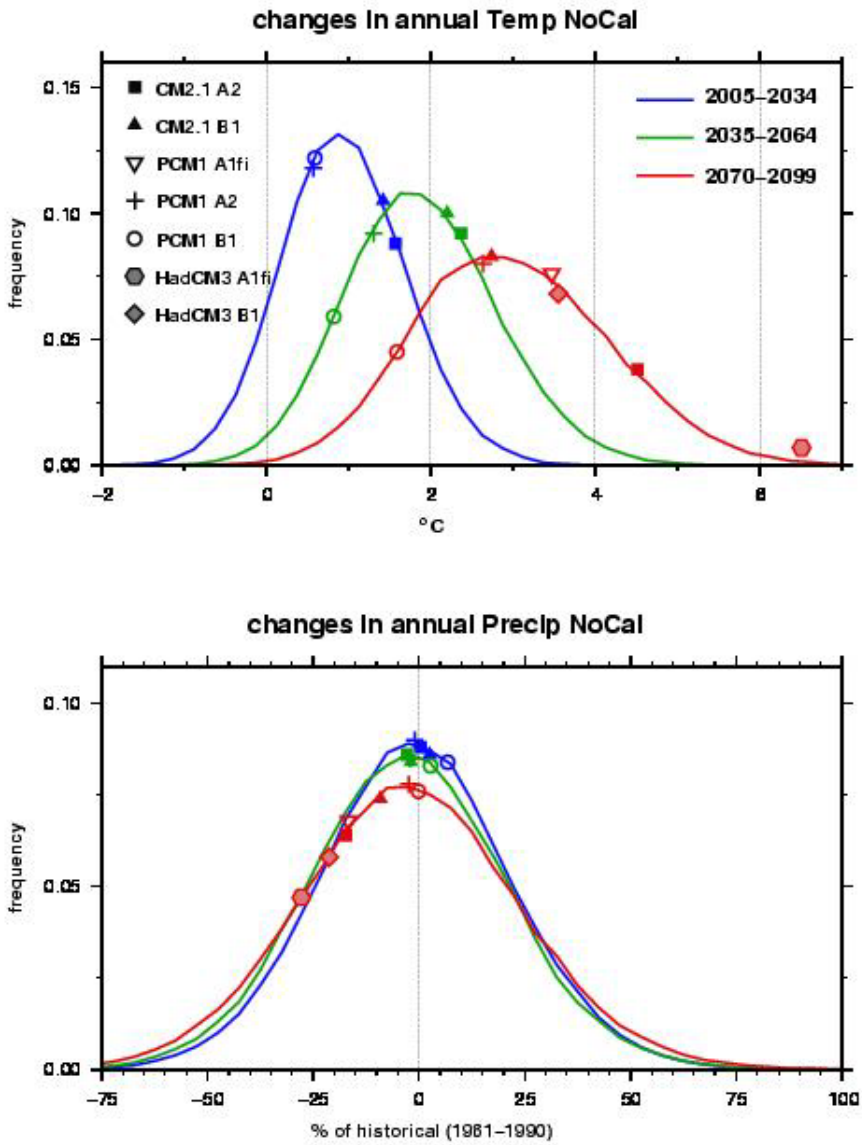

Figure 11. Distribution of changes in Northern California temperature (in ºC, above) and precipitation (in %, below) constructed from a sampling technique (Dettinger 2005) applied to recent set of IPCC 4th Assessment climate simulations, 13 models, 3 GHG emission scenarios). The temperature change plot shows that, by 2070-2099, virtually all simulations experience warming, by a broad range of amounts, but with a mean value of about +3C. On the other hand, concerning precipitation there are nearly as many simulations that become wetter as those that become drier, although by 2070-2099, there is a slight concensus to become drier, with the mean and most frequent value of precipitation change to be a decrease of just a few percent of its historical mean. Distributions are shown for 3 time blocks: 2005-2034, 2035-2064, and 2070-2099. The changes exhibited by the PCM and GFDL A2 and B1 simulations used in this study are indicated, for comparison with the entire family of climate projections.

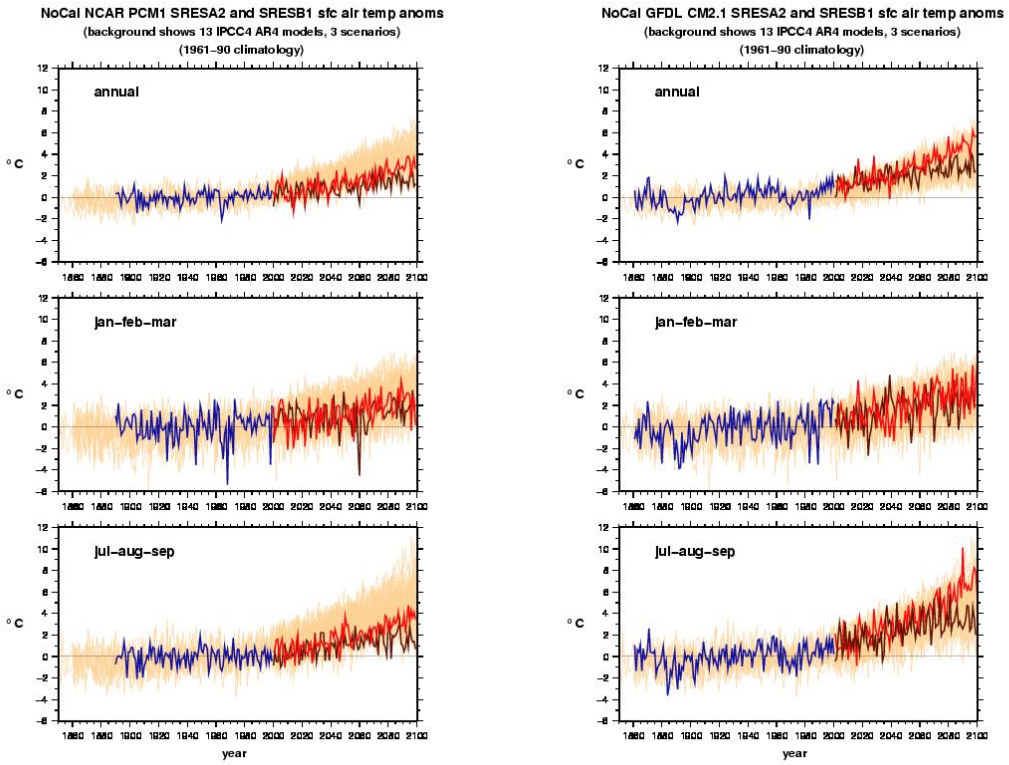

Figure 12a. Ensemble of Northern California temperature projections from 39 AR4 model simulations with PCM (left) and GFDL (right) B1 and A2 runs highlighted Note that models are coupled ocean atmosphere GCM's, and while they are driven by external forcings such as solar variability, volcanic aerosols, greenhouse gases and anthopogenic aerosols, they are not guided by ocean surface temperature or atmospheric circulation patterns that would allow them to replicate the actual observed climate variability during the historical period.

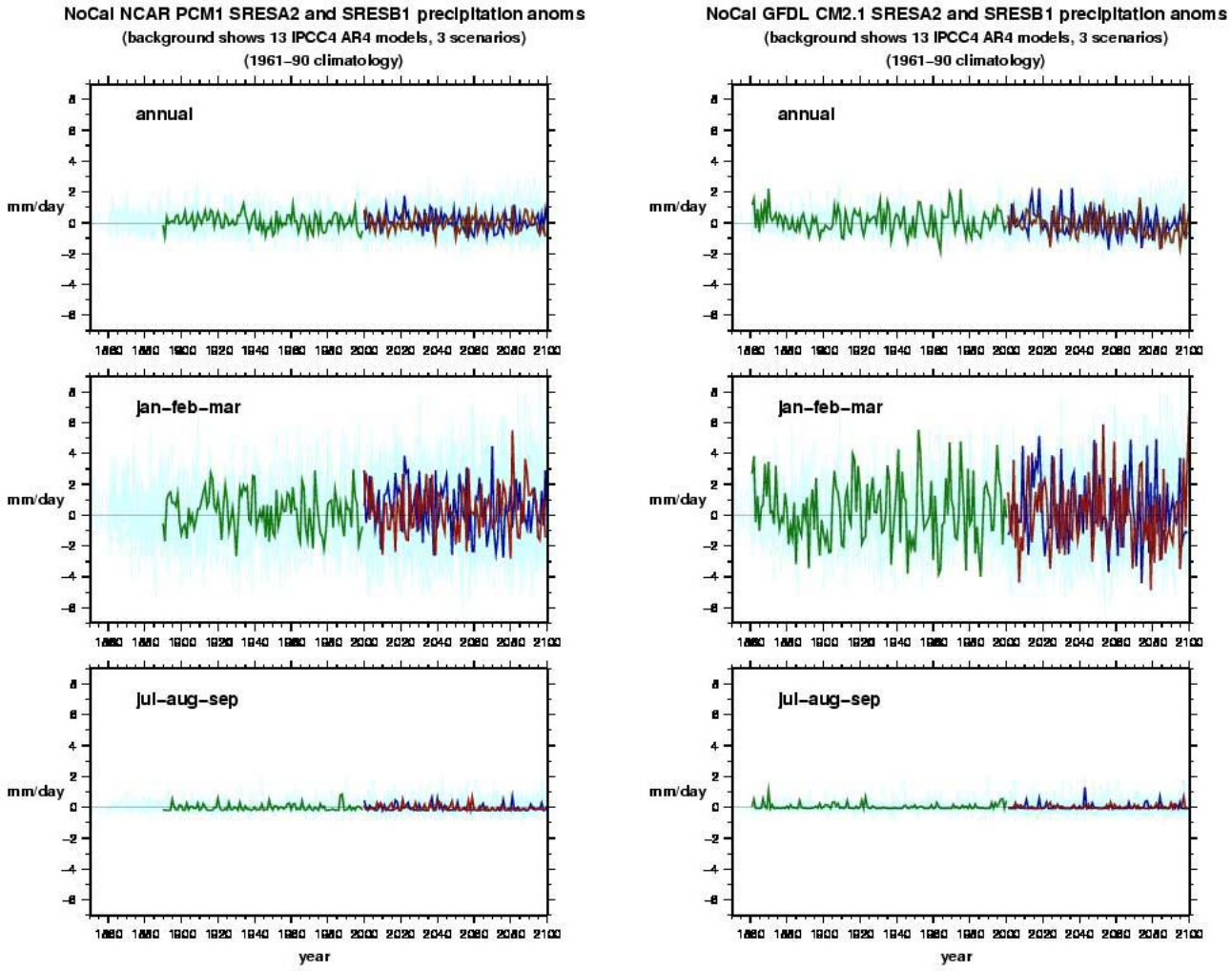

Figure 12b. Ensemble of Northern California precipitation projections from 39 AR4 model simulations with PCM (left) and GFDL (right) B1 and A2 runs highlighted

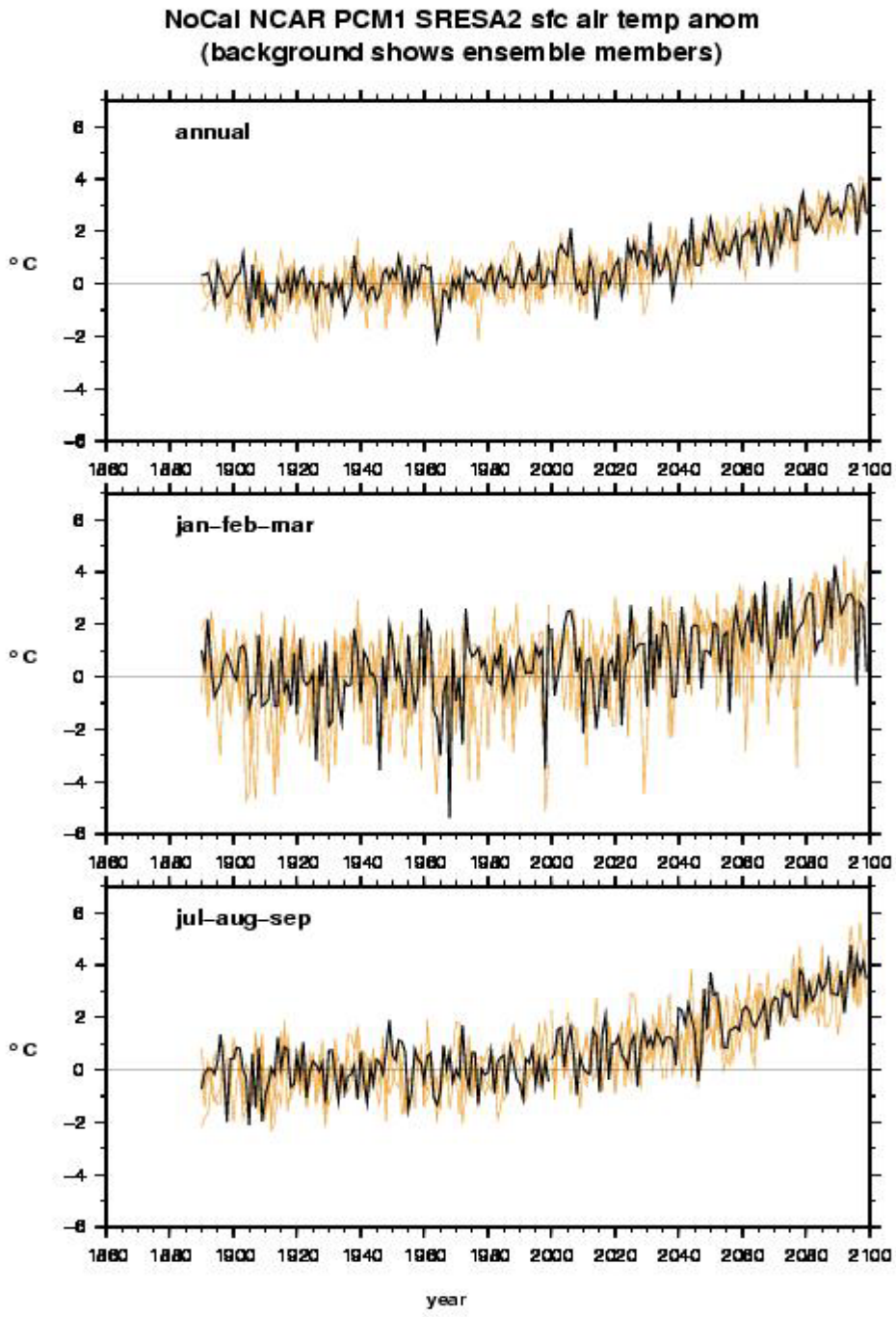

Figure 13a. Northern California Temperature Variability between four ensemble members, PCM A2 simulations, with simulation used in this study highlighted.

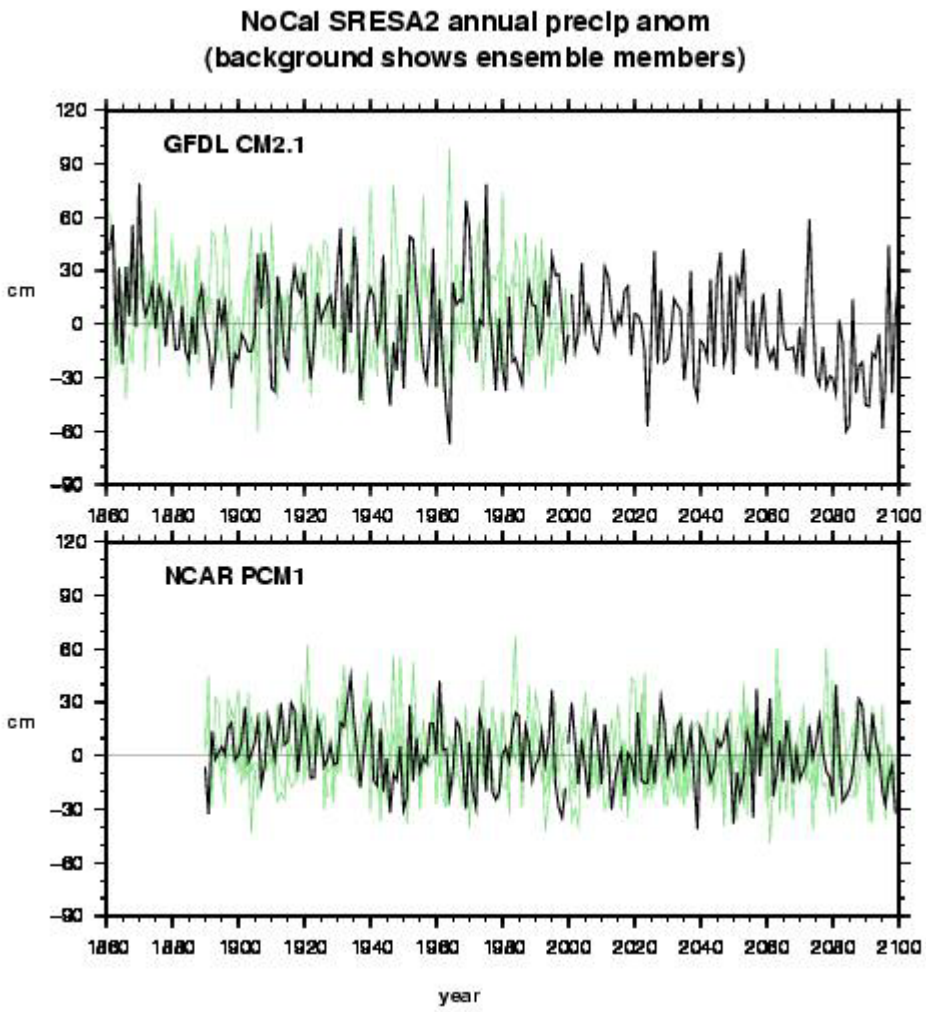

Figure 13b. Northern California Precipitation Variability between four ensemble members, GFDL A2 simulations, with simulation used in this study highlighted

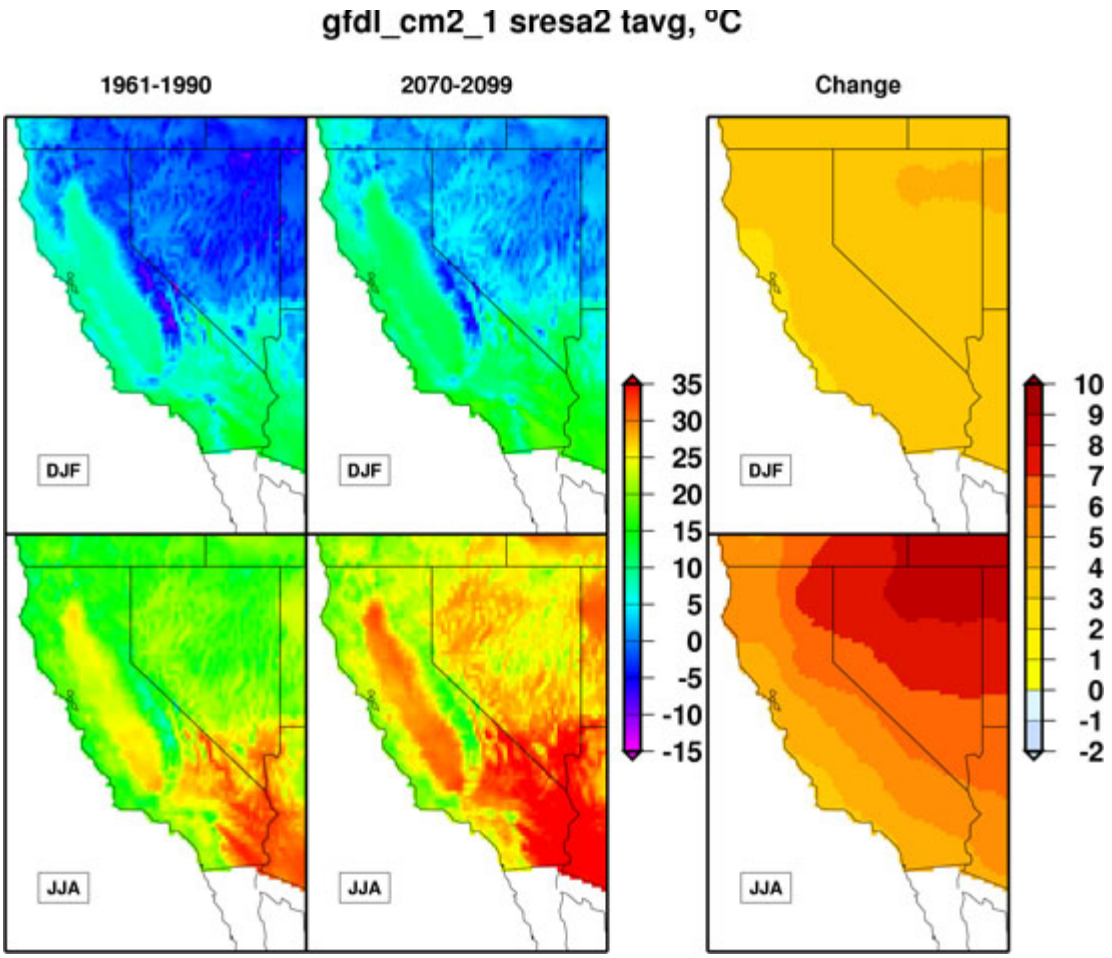

Figure 14. Temperature change from GFDL A2 simulation (right), and downscaled temperatures for (1961-1990) and (2070-2099) using Wood et al. statistical scheme (left).

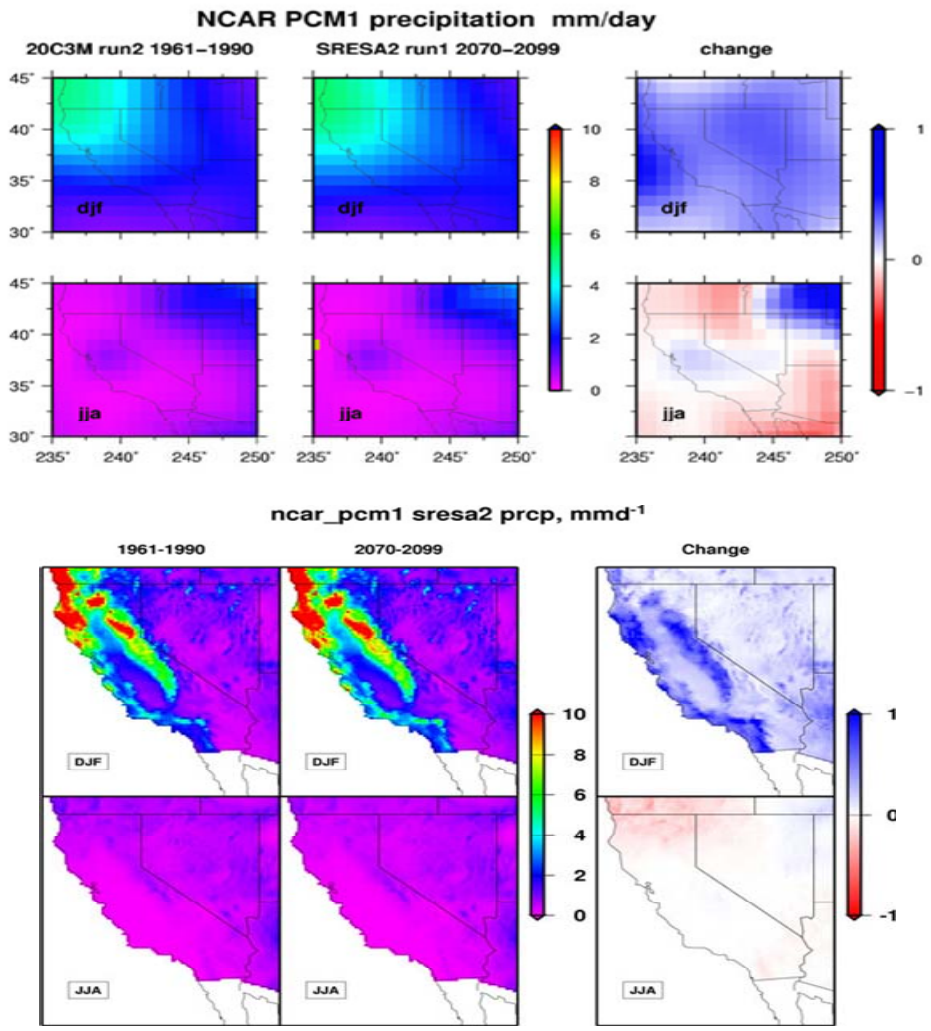

Figure 15. California precipitation 2070-2099, 1961-1990 and change from PCM (above) and high resolution representation from VIC statistical downscaling (below) for JJA and DJF.

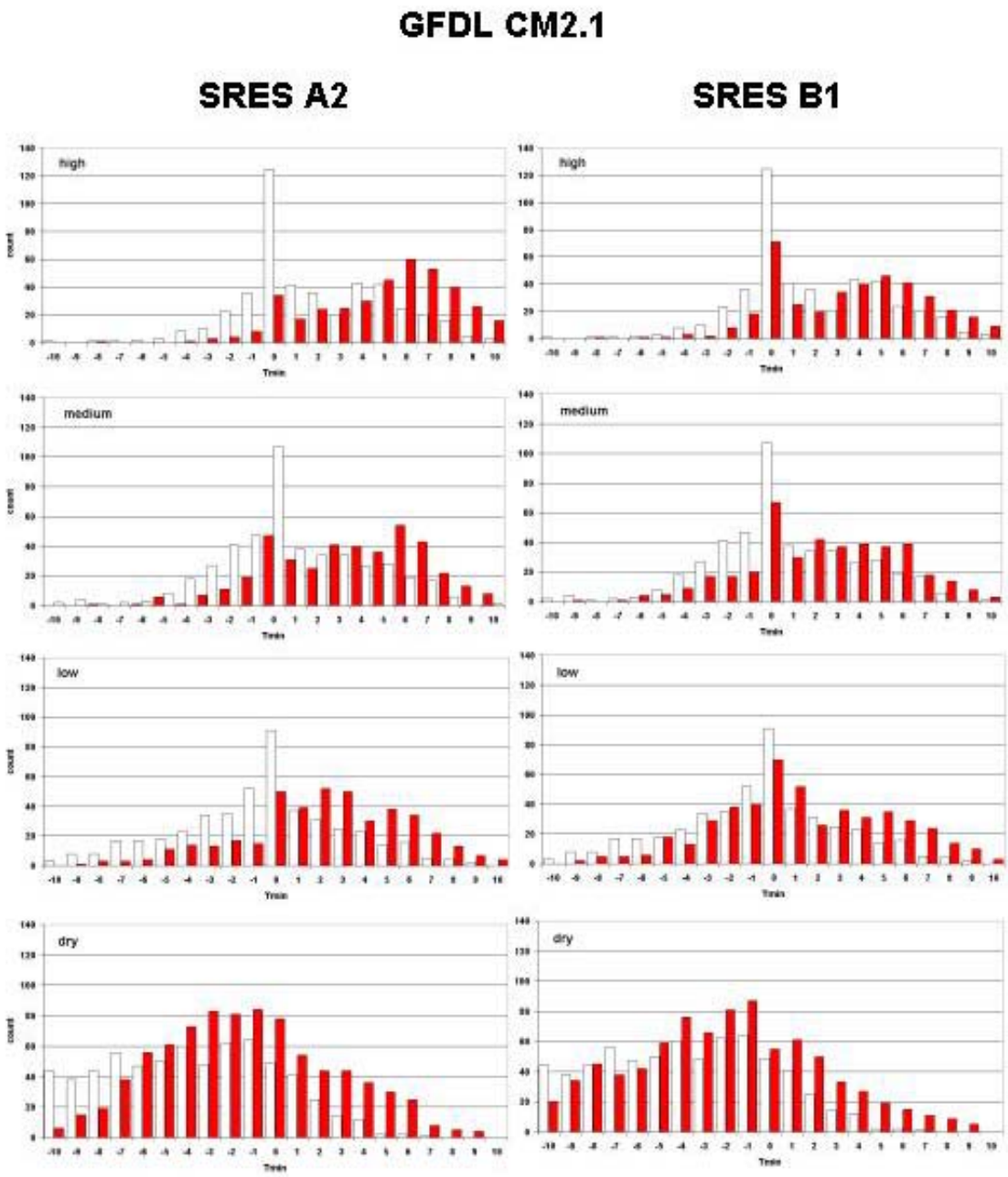

Figure 16. Distribution, binned by 1ºC intervals, of daily minimum temperature (Tmin) on days when precipitation is in upper, middle, lower tercile of daily precipitation amounts that exceed "drizzle" category, in addition to days with zero precipitation from GFDL A2 (left) and B1 (right) simulations. Open and red bars show contribution to frequency distributions from historical (1961-1990) and (2070-2099) periods, respectively. Frequency bins lower than -10C and greater than +10ºC are omitted.

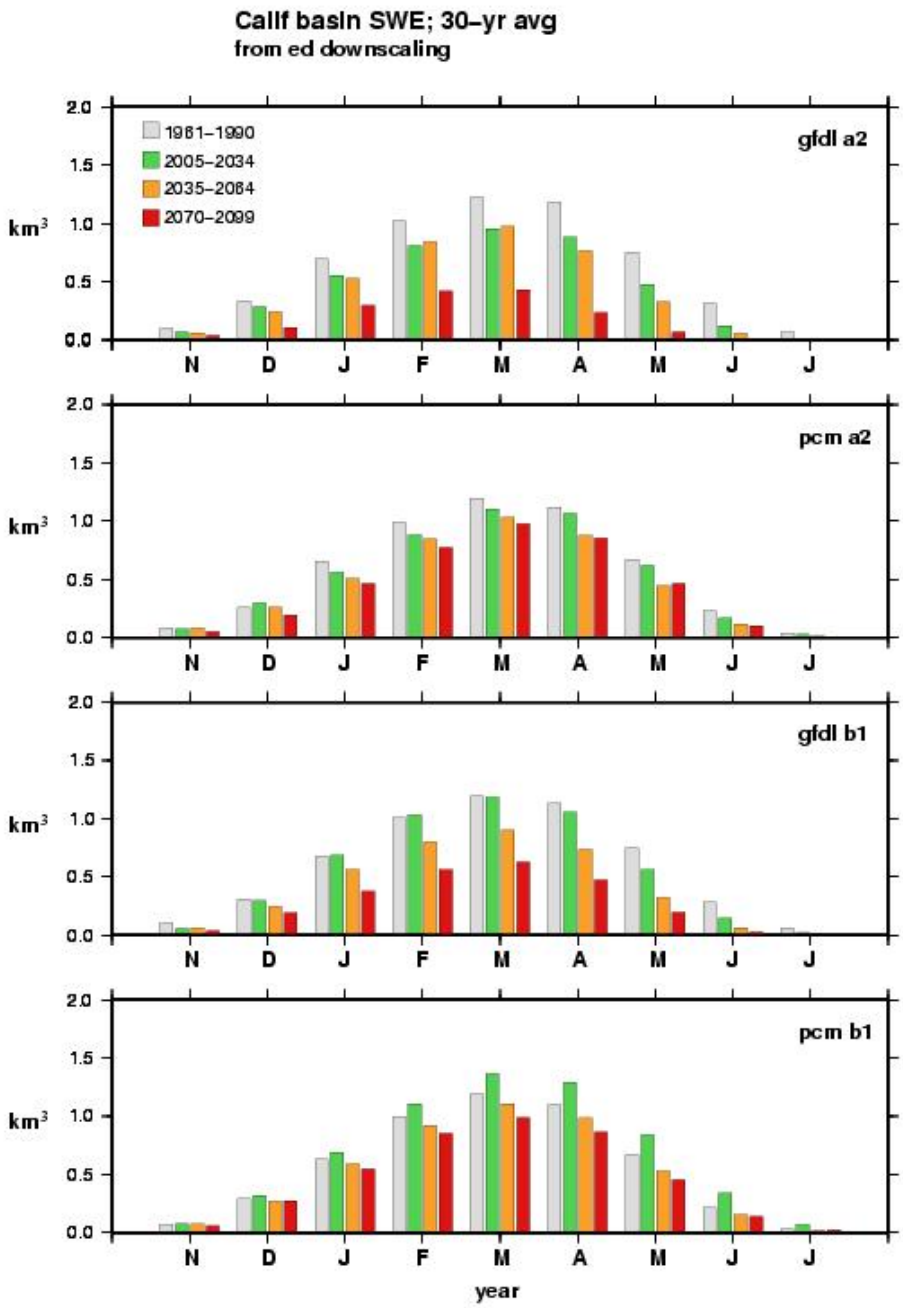

Figure 17. California Statewide April 1 Snow Water Equivalent Averages from Historical, 2005-2034, 2035-2064, 2070-2099 GFDL A2, PCM A2, GFDL B1 and PCM B1 simulations

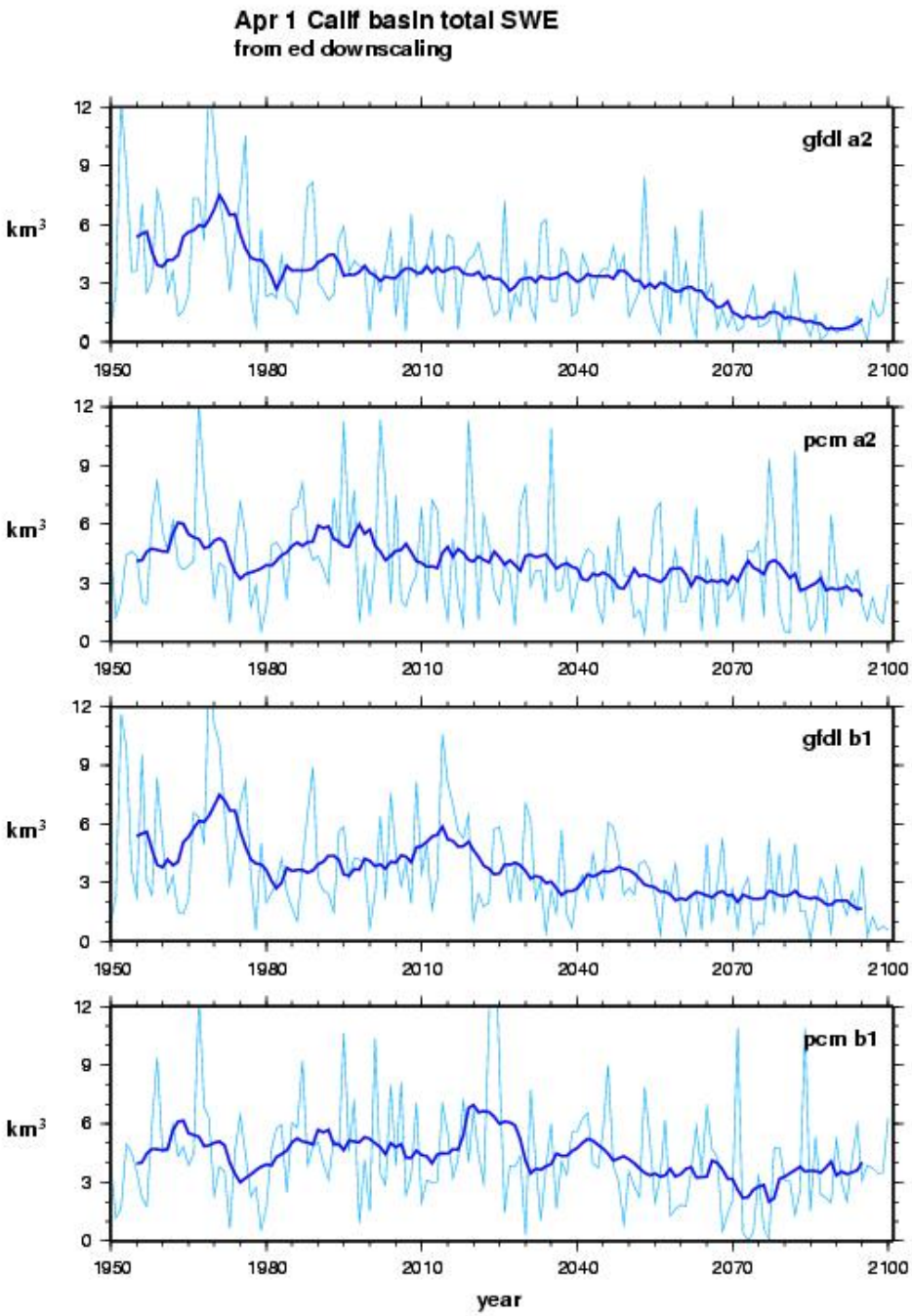

Figure 18. California Statewide April 1 Snow Water Equivalent GFDL A2, PCM A2, GFDL B1 and PCM B1 simulations

April 1 Snow Water Equivalent

2070-2090 fraction of 1961-1990

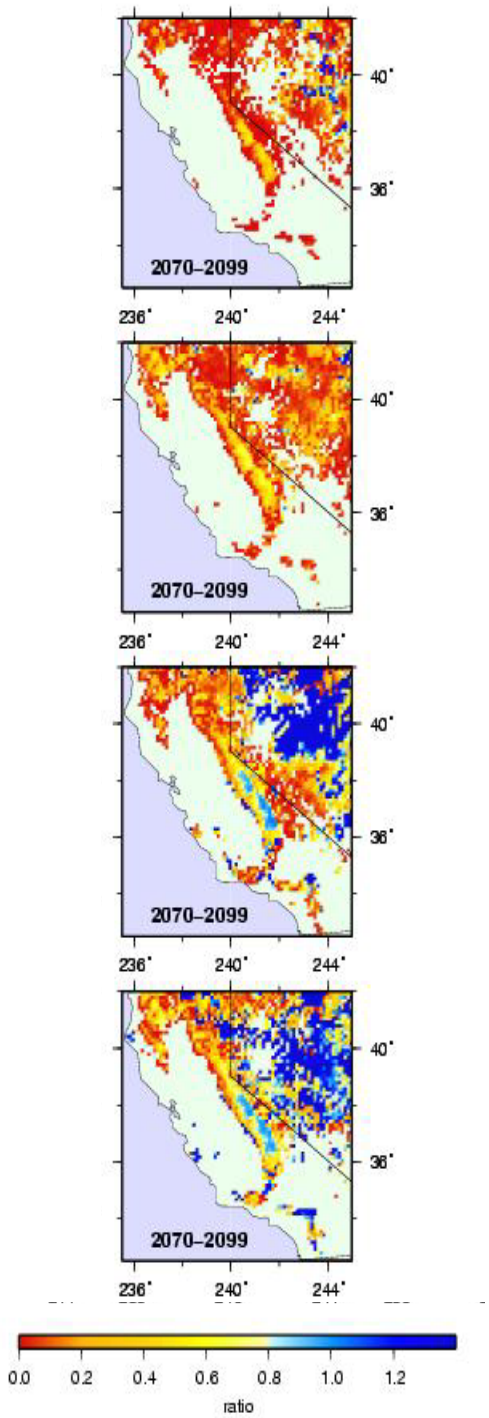

Figure 19. Change in spring snow accumulation from VIC, as driven by climate changes from four different climate change simulations. Changes are expressed as. ratio of 2070-2099 April 1 snow water equivalent (SWE) to that of historical (1961-1990).